AN H(div, Ω)-CONFORMING FLUX RECONSTRUCTION FOR THE MULTISCALE HYBRID-MIXED METHOD

Gabriel R Barrenechea, Larissa Martins, Weslley Pereira, Frederic Valentin

AN $H(\mathbf{div}, \Omega)$-CONFORMING FLUX RECONSTRUCTION FOR THE MULTISCALE HYBRID-MIXED METHOD

GABRIEL R. BARRENECHEA, LARISSA MARTINS, FRÉDÉRIC VALENTIN, AND FRÉDÉRIC VALENTIN

Abstract. The Multiscale Hybrid-Mixed (MHM) method is a multiscale finite element method based on a hybrid weak formulation, originally proposed for problems linked to flow in porous media. Its starting point is a variational formulation that guarantees that the flux variable is $H(\mathrm{div}, \Omega)$-conforming, but this property is lost when the local problems, in their elliptic form, are discretized using standard finite element methods. In this work, we close that gap by proposing and analyzing a new flux reconstruction, computed element-wise, that belongs to $H(\mathrm{div}, \Omega)$ for the MHM method. This reconstruction converges optimally in the $L^2(\Omega)$-norm, and its divergence is the projection onto the finite element space of the right-hand side datum of the problem, and thus it is super-convergent. As a by-product of the reconstruction technique, a fully computable *a posteriori* error estimator is presented and analyzed. These theoretical results are validated experimentally via numerical computations.

1. Introduction

Multiscale finite element methods have seen significant advancements in recent decades, both theoretically and practically. They are known for their accuracy on coarse meshes and their ability to efficiently utilize the new generation of massively parallel computers. Since the seminal work [7], there has been vast literature on the subject. In the context of the Darcy model (or Poisson equation) only, several alternatives have been proposed over the last two decades, such as the VMS method [28], MsFEM and GMsFEM [18], the PGEM and GEM [8, 23], the HMM [1], Multiscale Mortar method [6], the LOD method [33], the LSD method [32], just to cite a few (see, e.g., [31] for a recent review). This work focuses on the Multiscale Hybrid-Mixed (MHM for short) method [26, 4]. The MHM method is a byproduct of a hybrid formulation that starts at the continuous level posed on a coarse partition. It consists of decomposing the exact solution into local and global contributions. When discretized, such a characterization decouples local and global problems: the global formulation involves only degrees of freedom over the skeleton of the coarse partition, while the local problems provide the multiscale basis functions. Interestingly, the multiscale basis functions can be computed locally through independent problems. The local solvers can be done using primal finite element methods, as in [25, 9], or using mixed methods such as in [17]. The two-level MHM method [25, 9] is computationally attractive but it fails to preserve the $H(\mathrm{div}, \Omega)-$conformity presented in [17].

Fluxes or stresses often constitute the primary variables of interest in various applications, including heat conduction, percolation in porous media, and stress analysis [30]. An unresolved issue prompting further exploration pertains to the ability to perform an accurate $H(\mathrm{div}, \Omega)$ flux reconstruction using the discrete solution [21]. This form of post-processing holds significance in at least two scenarios: firstly, the flux can serve as crucial input data for subsequent calculations, as seen in the case of addressing contaminant transport issues in porous media where determining the flow velocity relies on an approximation

of Darcy's equation; secondly, the flux can be utilized in *a posteriori* error estimates reliant on equilibrated fluxes [21]. Consequently, in applications such as porous media flow, where $\boldsymbol{\sigma} = -A\nabla u$ denotes the Darcy velocity, it is important that this flux, in addition to being accurate, belongs to $H(\mathrm{div}, \Omega)$ (see, e.g., [15] for an example). This last requirement is of importance, on the one hand, because the continuity of the normal components of the flux guarantees conservation, and on the other, because the normal component of the flux is the natural input to model the transport phenomena.

The classical way of obtaining an accurate flux variable is by introducing a mixed (or hybrid) formulation of the problem and solve using appropriate mixed finite element methods. In the context of the MHM method, this results in the solution of mixed local problems (see [17]) with the associated increase of the computational cost for the local problems. In this work we take an alternative path, based on the works [13, 15], where an $H(\mathrm{div}, \Omega)-$conforming flux is built starting from the solution from the primal hybrid formulation. This recovered flux was built using the local Raviart-Thomas spaces (c.f. [35]). The reconstructed flux has continuous normal components and is conservative, even though the construction is carried out locally [13]. In the case of discontinuous Galerkin methods, an $H(\mathrm{div}, \Omega)$ flux reconstruction is proposed in [21]. So, in this work we build up on the ideas presented in the above-cited papers and propose, for the MHM method, a local flux reconstruction based on the local Raviart-Thomas space, and that produces a discrete flux variable, denoted by $\boldsymbol{\sigma}_h$, that belongs to $H(\mathrm{div}, \Omega)$. The presence of the submeshes associated with the skeleton of the global partition and local problems in the MHM method makes the extension nontrivial, as special care needs to be taken to guarantee the normal continuity in the interior facets of the subtriangulation (that is, the ones that do not have global degrees of freedom associated to them) while it maintains the MHM's accuracy. Due to the local character of the reconstruction, the computational overhead is negligible, while it produces an optimally converging flux in the $L^2(\Omega)$-norm. In addition, thanks to the nature of the MHM method, we prove that the divergence of the reconstructed flux is the projection of the right-hand side datum onto the finite element space used in the second-level computation. Hence, the projection of the divergence of $\boldsymbol{\sigma}_h$ super-converges.

As it was said earlier, flux reconstructions have been linked to the development of *a posteriori* error estimators. Up to our best knowledge, the first *a posteriori* error estimator that used this idea was proposed in [37], and similar ideas have been applied since in different contexts, e.g. [20, 12]. The main component of the estimators built in this way is the norm of the difference between the gradient of the primal variable and the reconstructed flux variable. So, in the last part of this work we use the recovered flux variable, combined with the general approach presented in [20], to derive a fully computable *a posteriori* error estimator for the MHM method. That is, a computable quantity that is a strict upper bound for the discretization error in the primal variable, while it is also a lower bound for the total discretization error.

The rest of the paper is organized as follows. In Section 2 the main notations, model problem, and preliminary results are presented. The MHM method is presented in Section 3, and the flux recovery is presented and analyzed in Section 4. In Secion 5 we derive the posteriori error estimator, and numerical experiments validating the theoretical results are given in Section 6. Some conclusions are drawn in Section 7, and in Appendix A we prove some technical results needed for the error analysis.

2. Setting and Preliminary Results

This section introduces the model problem and its hybrid formulation, and a characterization of the exact solution with respect to the solution of global-local boundary value problems. It follows closely previous works on the MHM method [4, 9].

2.1. **The Darcy model.** Let $\Omega \subset \mathbb{R}^d$, $d \in \{2, 3\}$, be an open, bounded, and connected polytope with Lipschitz boundary $\partial\Omega$. Given $f \in L^2(\Omega)$ and $g \in H^{1/2}(\partial\Omega)$, this work aims at approximating the following boundary value problem: Find $u \in H^1(\Omega)$ such that $u|_{\partial\Omega} = g$ and

$$\int_\Omega A\nabla u \cdot \nabla v = \int_\Omega f\, v \quad \text{for all } v \in H^1_0(\Omega)\,. \tag{2.1}$$

Here, $A \in L^\infty(\Omega)^{d\times d}$ is a symmetric matrix and may involve *multiscale* features. It is supposed to be uniformly elliptic in Ω. More precisely, we assume that there exist positive constants $A_{\min}$ and $A_{\max}$ such that

$$A_{\min}|\boldsymbol{\xi}|^2 \le \boldsymbol{\xi}^T A(\boldsymbol{x})\boldsymbol{\xi} \le A_{\max}|\boldsymbol{\xi}|^2 \quad \text{for all } \boldsymbol{\xi} \in \mathbb{R}^d\,, \tag{2.2}$$

and for almost all $\boldsymbol{x} \in \Omega$, where $|\cdot|$ is the Euclidian norm. The standard weak formulation (2.1) is a well-posed problem (c.f. [19, Example 25.4]).

Above and hereafter we will adopt standard notation for Sobolev and Lebesgue spaces aligned with, e.g., [19], where $H^m(D)$ ($L^2(D) = H^0(D)$) stands for the usual Sobolev spaces on an open bounded set $D \subset \mathbb{R}^d$, $d \in \{1, 2, 3\}$. We also denote by $(\cdot,\cdot)_D$ the $L^2(D)$-inner product (we do not make a distinction between vector-valued and scalar-valued functions), i.e.,

$$(f, g)_D = \int_D f\, g\,.$$

Finally, the product $\langle\cdot,\cdot\rangle_{\partial D}$ denotes the duality pairing between $H^{-1/2}(\partial D)$ and $H^{1/2}(\partial D)$, and we define the norms

$$\|\mu\|_{-1/2,\partial D} := \sup_{v\in H^{1/2}(\partial D)} \frac{\langle \mu, v\rangle_{\partial D}}{\|v\|_{1/2,\partial D}} \quad \text{and} \quad \|v\|_{1/2,\partial D} := \inf_{\substack{w\in H^1(D)\\ w=v \text{ on } \partial D}} \|w\|_{1,D}\,. \tag{2.3}$$

2.2. **Hybridization.** Following closely the presentation in [9], we start introducing $\mathscr{P}$, a collection of closed, bounded, disjoint polytopes, K, such that $\bar\Omega = \cup_{K\in\mathscr{P}} K$. The shapes of the polytopes K are, *a priori*, arbitrary, but we suppose that they satisfy a minimal angle condition (see Assumption A, Subsection 3.1, for a more precise statement). The diameter of K is $\mathcal{H}_K$ and we denote $\mathcal{H} = \max_{K\in\mathscr{P}} \mathcal{H}_K$. For each $K \in \mathscr{P}$, $\boldsymbol{n}^K$ denotes the unit outward normal to ∂K, such that $\boldsymbol{n}^K = \boldsymbol{n}$ on $\partial\Omega$ where $\boldsymbol{n}$ is the unit outward normal to $\partial\Omega$. We also introduce $\partial\mathscr{P}$ as the set of boundaries ∂K, $\mathcal{E}$ the set of the faces in $\mathscr{P}$, and $\mathcal{E}_0$ the set of internal faces. By $\boldsymbol{n}_E$ we denote a unit normal vector on faces $E \in \mathcal{E}$, and $\boldsymbol{n}^K_E$ the unit outward normal vector on E with respect to K.

Now, given a regular partition $\mathscr{P}$ of Ω, for $m \ge 1$ we define the broken Sobolev space

$$H^m(\mathscr{P}) := \{v : v|_K \in H^m(K), \forall\, K \in \mathscr{P}\} \text{ with norm } \|v\|^2_{m,\mathscr{P}} := \sum_{K\in\mathscr{P}} \|v\|^2_{m,K}\,.$$

In addition, the following spaces will be useful in what follows

$$V := H^1(\mathscr{P})\,,$$
$$V_0 := \{v \in V \,:\, v|_K \in \mathbb{P}_0(K) \text{ for all } K \in \mathscr{P}\}\,,$$

where $\mathbb{P}_0(K)$ stands for the space of constants functions in K,

$$\tilde{V} := \{v \in V \,:\, v|_K \in H^1(K) \cap L^2_0(K),\, K \in \mathscr{P}\}\,,$$

where $L^2_0(K)$ is the space function $L^2(K)$ with zero mean value functions. In addition, we define

$$\Lambda := \{\boldsymbol{\tau}\cdot\boldsymbol{n}^K|_{\partial K} \,:\, \boldsymbol{\tau} \in H(\mathrm{div},\Omega) \text{ for all } K \in \mathscr{P}\}\,.$$

Over the spaces V and Λ we define the respective norms

$$\|v\|_V = \left\{\sum_{K\in\mathscr{P}} \|v\|^2_{1,K}\right\}^{1/2} \text{ and } \|\mu\|_\Lambda = \inf_{\substack{\boldsymbol{\tau}\in H(\mathrm{div},\Omega)\\ \boldsymbol{\tau}\cdot\boldsymbol{n}^K=\mu \text{ on } \partial K}} \|\boldsymbol{\tau}\|_{\mathrm{div},\Omega}\,, \tag{2.4}$$

where $H(\mathrm{div},\Omega) := \{\boldsymbol{\tau} \in L^2(\Omega)^d \,:\, \nabla\cdot\boldsymbol{\tau} \in L^2(\Omega)\}$ with norm

$$\|\boldsymbol{\tau}\|_{\mathrm{div},\Omega} := \left\{\sum_{K\in\mathscr{P}} \|\boldsymbol{\tau}\|^2_{0,K} + \|\nabla\cdot\boldsymbol{\tau}\|^2_{0,K}\right\}^{1/2}\,. \tag{2.5}$$

Let $[\![v]\!]$ represents the jump of v on $E \in \mathcal{E}$, i.e., for two elements K and K' sharing E, we define

$$[\![v]\!]|_E := v|_K - v|_{K'} \quad \text{on } E \in \mathcal{E}_0\,, \tag{2.6}$$

and $[\![v]\!] := v$ on $E \subset \partial\Omega$. We also define $\{v\}$, the average value of v on $E \in \mathcal{E}$, as

$$\{v\} := \frac{1}{2}(v|_K + v|_{K'})\,, \tag{2.7}$$

where K, K' are neighboring elements and on $E \subset \partial\Omega$, $\{v\} := v$. We define the products on $\mathscr{P}$ and $\partial\mathscr{P}$ as

$$(v,w)_{\mathscr{P}} := \sum_{K\in\mathscr{P}} (v,w)_K \quad \text{and} \quad \langle\mu,v\rangle_{\partial\mathscr{P}} := \sum_{K\in\mathscr{P}} \langle\mu,v\rangle_{\partial K}\,. \tag{2.8}$$

We recall from [24] that

$$\|\mu\|_\Lambda = \sup_{v\in V} \frac{\langle\mu,v\rangle_{\partial\mathscr{P}}}{\|v\|_V} \quad \text{for all } \mu \in \Lambda\,. \tag{2.9}$$

We also define the following norm over the space $L^2(\partial\mathscr{P})$

$$\|\mu\|_\star = \left(\sum_{K\in\mathscr{P}} \mathcal{H}_K \|\mu\|^2_{0,\partial K}\right)^{1/2}\,. \tag{2.10}$$

We are ready to present a hybrid formulation for (2.1). Here we relax the continuity of u on the skeleton $\partial\mathscr{P}$ by introducing the Lagrange multiplier λ. The hybrid formulation reads: Find $(\lambda,u) \in \Lambda \times V$ such that

$$\begin{cases} (A\nabla u, \nabla v)_{\mathscr{P}} - \langle\lambda, v\rangle_{\partial\mathscr{P}} = (f,v)_{\mathscr{P}} & \text{for all } v \in V,\\ \langle\mu,u\rangle_{\partial\mathscr{P}} = \langle\mu,g\rangle_{\partial\Omega} & \text{for all } \mu \in \Lambda. \end{cases} \tag{2.11}$$

Observe that (2.11) is a saddle point problem wherein the exact solution u is sought in a space V larger than $H^1(\Omega)$. Nonetheless, the introduction of the Lagrange multiplier $\lambda \in \Lambda$, which ensures the weak continuity of u on $\mathscr{P}$, leads u to belong to $H^1(\Omega)$ and to satisfy the original formulation (2.1). These results were proved originally in [35] and extended in [9] to more general partitions $\mathscr{P}$.

2.3. **A characterization of the exact solution.** The exact solution of (2.1) can be characterized in terms of the solution to local and global problems. Following closely [4], we define the bounded mappings $T \in \mathcal{L}(\Lambda, V)$ and $\hat{T} \in \mathcal{L}(L^2(\Omega), V)$ as follows

- for all $\mu \in \Lambda$, $T\mu\,|_K \in H^1(K) \cap L^2_0(K)$ is the unique solution of

$$\int_K A\nabla T\mu \cdot \nabla v = \langle \mu, v\rangle_{\partial K} \quad \text{for all } v \in H^1(K) \cap L^2_0(K)\,,\ \forall\, K \in \mathscr{P}\,; \tag{2.12}$$

- for all $q \in L^2(\Omega)$, $\hat{T}q\,|_K \in H^1(K) \cap L^2_0(K)$ is the unique solution of

$$\int_K A\nabla \hat{T}q \cdot \nabla v = \int_K q\, v \quad \text{for all } v \in H^1(K) \cap L^2_0(K)\,,\ \forall\, K \in \mathscr{P}\,. \tag{2.13}$$

Hence, the solution of (2.1) can be written as

$$u = u_0 + T\lambda + \hat{T}f\,, \tag{2.14}$$

where $(\lambda, u_0) \in \Lambda \times V_0$ solves the following mixed problem

$$\begin{cases} \langle \mu, T\lambda\rangle_{\partial\mathscr{P}} + \langle \mu, u_0\rangle_{\partial\mathscr{P}} = -\langle \mu, \hat{T}f\rangle_{\partial\mathscr{P}} + \langle \mu, g\rangle_{\partial\Omega} & \text{for all } \mu \in \Lambda\,, \\ \langle \lambda, v_0\rangle_{\partial\mathscr{P}} = -(f, v_0)_{\mathscr{P}} & \text{for all } v_0 \in V_0\,. \end{cases} \tag{2.15}$$

The well-posedness of (2.15) was proved in [4, Section 3.1] for the partition of Ω into simplicial elements, and [9, Theorem 2.1] for more general cases.

3. The MHM method

This section presents the MHM method. Next, we introduce some notation needed to define the method in general polytopal meshes.

3.1. **Settings.** The MHM method uses a multi-level discretization starting from the first-level partition $\mathscr{P}$. Notably, each face $E \subset \mathcal{E}$ and polytopal element $K \in \mathscr{P}$ may carry its own family of partitions in a way that each member is *a priori* independent of each other [24]. We start discretizing the set of faces $E \in \mathcal{E}$. For this, let $\{\mathcal{E}_H\}_{H>0}$ be a family of partitions of $\mathcal{E}$, for which each $E \in \mathcal{E}$ is split into faces F of diameter $H_F \le H := \max_{F\in\mathcal{E}_H} H_F$.

Assumption A: The family of meshes $\{\mathcal{E}_H\}_{H>0}$ induces a shape regular family of simplicial triangulation $\{\Xi_H^K\}_{H>0}$ for each $K \in \mathscr{P}$, such that their trace on ∂K coincides with $\{\mathcal{E}_H\}_{H>0}$.

In addition, for each $K \in \mathscr{P}$, we introduce a shape regular family of simplicial triangulations $\{\mathscr{T}_h^K\}_{h>0}$ made up of simplices $T \in \mathscr{T}_h^K$ of diameter $h_T \le h := \max_{K\in\mathscr{P}} \max_{T\in\mathscr{T}_h^K} h_T$ (see Figure 1 for an illustration in two-dimensions). In each element $K \in \mathscr{P}$ the mesh $\mathscr{T}_h^K$ will be assumed to be a regular refinement of the triangulation Ξ_H^K. For $T \in \mathscr{T}_h^K$, let $\mathcal{F}_T$ denote the set of its facets, $\mathcal{F}_h^K$ the set of all facets of $\mathscr{T}_h^K$, and $\mathcal{F}_0^K \subset \mathcal{F}_h^K$ the set of facets internal to K. For $\mathfrak{f} \in \mathcal{F}_T$, $h_\mathfrak{f}$ denotes its diameter. We note that every $\mathfrak{f} \in \mathcal{F}_T \cap \partial K$ is included in one, and only one $F \in \mathcal{E}_H$.

For $k, \ell \ge 0$ we define the following finite element spaces associated to $\mathcal{E}_H$ and $\mathscr{T}_h^K$

$$\Lambda_H := \{\mu_H \in \Lambda : \mu_H|_F \in \mathbb{P}_\ell(F),\ \forall\, F \in \mathcal{E}_H\}\,, \tag{3.1}$$

$$V_h^k := \prod_{K\in\mathscr{P}} V_h^k(K)\,, \tag{3.2}$$

$$\tilde{V}_h := \prod_{K\in\mathscr{P}} \tilde{V}_h(K) \ \text{ where } \ \tilde{V}_h(K) := V_h^k(K) \cap L^2_0(K)\,, \tag{3.3}$$

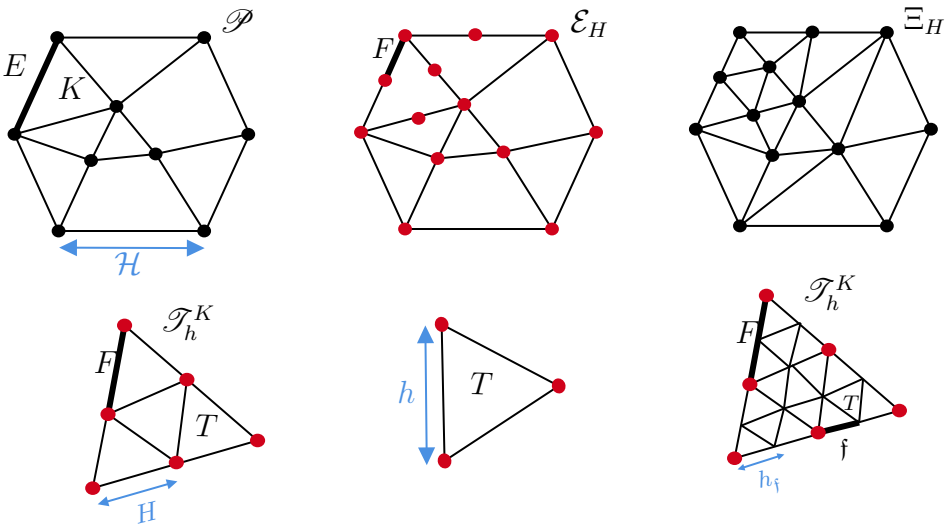

FIGURE 1. A polytopal domain $\mathscr{P}$ discretized with conforming elements K (upper left). The mesh $\mathcal{E}_H$ is defined over the skeleton of $\mathscr{P}$ (upper center). Ξ_H is a simplicial mesh (upper right) that matches $\mathcal{E}_H$. A minimal (bottom left) and a refined (bottom right) submesh in element K and a simplex T (bottom center). The black dots represent the degrees of freedom associated with Ξ_H and the red dots with the mesh skeleton.

where

$$V_h^k(K) := \{v_h \in C^0(K) \,:\, v_h|_T \in \mathbb{P}_k(T),\, \forall\, T \in \mathscr{T}_h^K\}\,, \quad \text{for } k \geq 1\,, \tag{3.4}$$

and $V_h^0(K) := \mathbb{P}_0(K)$.

Now, we introduce local projections onto more general piecewise polynomial spaces. For $K \in \mathscr{P}$, $m \geq 0$, we introduce the operator $\Pi_{K,m} : L^1(K) \to V_h^m(K)$ such that

$$\int_K \Pi_{K,m}(g) v = \int_K g\, v \quad \text{for all } v \in V_h^m(K)\,, \tag{3.5}$$

and the global projection $\Pi_{\Omega,m}$ such that $\Pi_{\Omega,m}(\cdot)|_K = \Pi_{K,m}(\cdot)$. Also, we define, for $T \in \mathscr{T}_h^K$, the operator $\boldsymbol{\Pi}_{T,m} : L^1(T)^d \to \mathbb{P}_m(T)^d$ as

$$\int_T \boldsymbol{\Pi}_{T,m}(\boldsymbol{g}) \cdot \boldsymbol{v} = \int_T \boldsymbol{g} \cdot \boldsymbol{v} \quad \text{for all } \boldsymbol{v} \in \mathbb{P}_m(T)^d\,. \tag{3.6}$$

In addition, for $F \in \mathcal{E}_H$, we define the projection operator $\Pi_{F,m} : L^1(F) \to \mathbb{P}_m(F)$ such that

$$\int_F \Pi_{F,m}(\mu)\xi = \int_F \mu\, \xi \quad \text{for all } \xi \in \mathbb{P}_m(F)\,, \tag{3.7}$$

and the global projection operator $\Pi_{\mathcal{E},m}$ as $\Pi_{\mathcal{E},m}(\cdot)|_F = \Pi_{F,m}(\cdot)$.

3.2. **The MHM method.** Using the finite element spaces defined in (3.1)-(3.3) and $k \geq \ell + d$, the discrete equivalents of the mappings T and $\hat{T}$ defined in (2.12)-(2.13) read

- for all $\mu \in \Lambda$, $T_h\mu \in \tilde{V}_h$ is the unique solution of

$$\int_K A\nabla T_h\mu \cdot \nabla v_h = \langle \mu, v_h\rangle_{\partial K} \quad \text{for all } v_h \in \tilde{V}_h(K) \quad \text{and} \quad K \in \mathscr{P}\,; \tag{3.8}$$

- for all $q \in L^2(\Omega)$, $\hat{T}_h q \in \tilde{V}_h$ is the unique solution of

$$\int_K A\nabla \hat{T}_h q \cdot \nabla v_h = \int_K q\, v_h \quad \text{for all } v_h \in \tilde{V}_h(K) \quad \text{and} \quad K \in \mathscr{P}\,. \tag{3.9}$$

Using the discrete mappings (3.8)-(3.9), the discrete version of the problem (2.15) is: Find $(\lambda_H, u_0^h) \in \Lambda_H \times V_0$ such that

(3.10)
$$\begin{cases} \langle \mu_H, T_h\lambda_H\rangle_{\partial\mathscr{P}} + \langle \mu_H, u_0^h\rangle_{\partial\mathscr{P}} = -\langle \mu_H, \hat{T}_h f\rangle_{\partial\mathscr{P}} + \langle \mu_H, g\rangle_{\partial\Omega} & \text{for all } \mu_H \in \Lambda_H\,, \\ \langle \lambda_H, v_0\rangle_{\partial\mathscr{P}} = -(f, v_0)_{\mathscr{P}} & \text{for all } v_0 \in V_0\,. \end{cases}$$

The approximate solution is given by

$$u_{Hh} := u_0^h + T_h\lambda_H + \hat{T}_h f\,. \tag{3.11}$$

For the well-posedness of the MHM method, see [9, Theorem 2] and for a general case [24, Theorem 4.4].

Next, we present *a priori* error estimates for the MHM method. Hereafter, we denote by C a positive constant independent of mesh sizes, which may depend on physical coefficients $A_{\min}$ and $A_{\max}$.

Theorem 3.1. *Let us assume that u, solution of the hybrid formulation, belongs to $H^{k+1}(\mathscr{P})$ and $A\nabla u \in H^{\ell+1}(\mathscr{P}) \cap H(div,\Omega)$, with $\ell \geq 0$ and $k \geq \ell + d$. Then, there exists C such that*

$$\|u_0 - u_0^h\|_V + \|\lambda - \lambda_H\|_\Lambda \leq C\,\left(h^k|u|_{k+1,\mathscr{P}} + H^{\ell+1}|A\nabla u|_{\ell+1,\mathscr{P}}\right)\,.$$

In addition, if u_{Hh} is given in (3.11)*, then the following error estimate holds*

$$\|u - u_{Hh}\|_V \leq C\,\left(h^k|u|_{k+1,\mathscr{P}} + H^{\ell+1}|A\nabla u|_{\ell+1,\mathscr{P}}\right)\,.$$

Proof. For details, see [9, Theorem 3]. □

4. Post-processing for the dual variable for MHM

To develop the flux recovery strategy from the solution of the MHM method (3.10), we need to build subspaces of finite dimension of $H(\mathrm{div},\Omega)$. Among the most renowned approximation spaces in the literature for $H(\mathrm{div},\Omega)$ are the Raviart-Thomas spaces. In this section, we propose to construct a $\boldsymbol{\sigma}_h$ in a way that its normal component is continuous on the interelement boundary, i.e., $\boldsymbol{\sigma}_h \in H(\mathrm{div},\Omega)$, through the definition of new local problems.

4.1. The Raviart-Thomas space.

Following [16, Chapter 3] we will build a Raviart-Thomas space in the submesh $\mathscr{T}_h^K$, which is a simplicial mesh, and assume the same properties of the Raviart-Thomas space in those meshes.

First, we introduce the local spaces. Given a simplex $T \subseteq \mathbb{R}^d$, the local Raviart-Thomas space of order $m \geq 0$ is defined by

$$\mathcal{RT}_m(T) = \mathbb{P}_m(T)^d + \boldsymbol{x}\mathbb{P}_m(T)\,, \tag{4.1}$$

and recall the Raviart-Thomas local interpolation operator

$$\pi_T^{\mathcal{RT}_m} : H^s(T)^d \to \mathcal{RT}_m(T)\,, \tag{4.2}$$

with $s > 1/2$, where, for $\boldsymbol{v} \in H^s(T)^d$, $\pi_T^{\mathcal{RT}_m}\boldsymbol{v} \in \mathcal{RT}_m(T)$ is the only element of the local Raviart-Thomas space satisfying

$$\int_{\mathfrak{f}_i} (\pi_T^{\mathcal{RT}_m}\boldsymbol{v}\cdot\boldsymbol{n}_{\mathfrak{f}_i}^T)\mu = \int_{\mathfrak{f}_i} (\boldsymbol{v}\cdot\boldsymbol{n}_{\mathfrak{f}_i}^T)\mu \quad \text{for all } \mu \in \mathbb{P}_m(\mathfrak{f}_i)\,,\ i = 1,\cdots,d+1\,, \tag{4.3}$$

and if $m \geq 1$,

$$\int_T \pi_T^{\mathcal{RT}_m}\boldsymbol{v}\cdot\boldsymbol{\tau} = \int_T \boldsymbol{v}\cdot\boldsymbol{\tau} \quad \text{for all } \boldsymbol{\tau} \in \mathbb{P}_{m-1}(T)^d\,. \tag{4.4}$$

The Raviart–Thomas interpolation has an optimal-order error estimate, namely, there exists a constant C depending on m, d, and the regularity constant of the mesh such that, for any $\boldsymbol{v} \in H^{m+1}(T)^d$,

$$\|\boldsymbol{v} - \pi_T^{\mathcal{RT}_m}\boldsymbol{v}\|_{0,T} \leq C\,h_T^{m+1}|\boldsymbol{v}|_{m+1,T}\,. \tag{4.5}$$

Associated with $\mathscr{T}_h^K$ we introduce the global space over $K \in \mathscr{P}$

$$\mathcal{RT}_m(\mathscr{T}_h^K) = \{\boldsymbol{v} \in H(\mathrm{div}, K) \,:\, \boldsymbol{v}|_T \in \mathcal{RT}_m(T)\,, \forall\, T \in \mathscr{T}_h^K\}\,. \tag{4.6}$$

An essential tool in error analysis is the operator

$$\pi_K^{\mathcal{RT}_m} : H(\mathrm{div}, K) \cap \prod_{T\in\mathscr{T}_h^K} H^s(T)^d \to \mathcal{RT}_m(\mathscr{T}_h^K)\,,$$

with $s > 1/2$, defined by

$$\pi_K^{\mathcal{RT}_m}\boldsymbol{v}|_T = \pi_T^{\mathcal{RT}_m}\boldsymbol{v} \qquad \text{for all } T \in \mathscr{T}_h^K\,. \tag{4.7}$$

As a consequence of its definition, the operator $\pi_K^{\mathcal{RT}_m}$ satisfies

$$\int_K \nabla\cdot(\boldsymbol{v} - \pi_K^{\mathcal{RT}_m}\boldsymbol{v})q = 0\,,$$

for all $\boldsymbol{v} \in H(\mathrm{div}, K) \cap \prod_{T\in\mathscr{T}_h^K} H^s(T)^d$ and all $q \in \{g \in L^2(K) \,:\, g|_T \in \mathbb{P}_m(T)\,, \forall\, T \in \mathscr{T}_h^K\}$, for every $K \in \mathscr{P}$. Moreover,

$$\nabla\cdot\mathcal{RT}_m(\mathscr{T}_h^K) = \{g \in L^2(K) : g|_T \in \mathbb{P}_m(T)\,, \forall\, T \in \mathscr{T}_h^K\}\,.$$

Also, in [19, Example 12.6], the following stability is proven: There exists $C > 0$, independent of $\mathcal{H}$, H, and h such that,

$$\|\boldsymbol{v}\|_{0,T} \le C\left(\|\boldsymbol{\Pi}_{T,m-1}(\boldsymbol{v})\|_{0,T} + h_T^{1/2}\max_{\mathfrak{f}\in\mathcal{F}_T}\|\boldsymbol{v}\cdot\boldsymbol{n}_\mathfrak{f}\|_{0,\mathfrak{f}}\right) \quad \forall\,\boldsymbol{v} \in \mathcal{RT}_m(T)\,, \tag{4.8}$$

where $\boldsymbol{\Pi}_{T,m-1}$ is defined in (3.6) with $m \ge 1$.

4.2. **Flux Recovery.** In this section we present the construction of the post-processed flux. Once the solution (λ_H, u_{Hh}) of the MHM method (3.10) is computed, we construct $\boldsymbol{\sigma}_h \in \mathcal{RT}_\ell(T)$ on each $T \in \mathscr{T}_h^K$, $\ell \ge 0$, as follows:

$$\begin{cases} \boldsymbol{\sigma}_h\cdot\boldsymbol{n}_\mathfrak{f} = -\lambda_H & \text{if } \mathfrak{f} \subset \partial T \cap \partial K\,,\\ \displaystyle\int_\mathfrak{f}(\boldsymbol{\sigma}_h\cdot\boldsymbol{n}_\mathfrak{f})\mu = \int_\mathfrak{f} -\{A\nabla u_{Hh}\}\cdot\boldsymbol{n}_\mathfrak{f}\,\mu & \text{for all } \mu \in \mathbb{P}_\ell(\mathfrak{f}),\ \text{if } \mathfrak{f} \in \mathcal{F}_0^K \cap \mathcal{F}_T\,,\\ \displaystyle\int_T \boldsymbol{\sigma}_h\cdot\boldsymbol{\tau} = \int_T -A\nabla u_{Hh}\cdot\boldsymbol{\tau} & \text{for all } \boldsymbol{\tau} \in \mathbb{P}_{\ell-1}(T)^d,\ (\ell \ge 1)\,, \end{cases} \tag{4.9}$$

where $\mathcal{F}_0^K \cap \mathcal{F}_T$ is the internal facet of T, $\boldsymbol{n}_\mathfrak{f}$ is a fixed unit outward normal to $\mathfrak{f}$. Note that, for $\ell = 0$, the third equation of (4.9) is not necessary.

Remark 4.1. *The post-processing technique presented in* (4.9) *generalizes the ones proposed in [13] and [15] to the case of a multiscale method with a submesh. In fact, the techniques coincide in the case $\mathscr{P}$ is a simplicial triangulation, and as submesh we only take one element per each K, that is, $\mathscr{T}_h^K = \{K\}$ and $\mathcal{H} = H = h$. In such a case, since there is not a submesh, the second equation in* (4.9) *is no longer present.*

By construction, we immediately obtain the following two results.

Proposition 4.1. *The normal components of $\boldsymbol{\sigma}_h$ are continuous across the interelement boundaries, i.e., we have $\boldsymbol{\sigma}_h \in H(div, \Omega)$.*

Proof. It follows from (2.6) that, if $\mathfrak{f} \subset \partial K \cap \partial T$, for two adjacent elements T, T' such that $\mathfrak{f} = \partial T \cap \partial T'$,

$$[\![\boldsymbol{\sigma}_h\cdot\boldsymbol{n}_\mathfrak{f}]\!]|_\mathfrak{f} = -\lambda_H|_T + \lambda_H|_{T'} = 0\,.$$

On the other hand, if $\mathfrak{f} \in \mathcal{F}_0^K \cap \mathcal{F}_T$, let $\mu \in \mathbb{P}_\ell(\mathfrak{f})$, then

$$\int_\mathfrak{f} [\![\boldsymbol{\sigma}_h\cdot\boldsymbol{n}_\mathfrak{f}]\!]\,\mu = -\int_\mathfrak{f}\{A\nabla u_{Hh}\}|_T\cdot\boldsymbol{n}_\mathfrak{f}\,\mu + \int_\mathfrak{f}\{A\nabla u_{Hh}\}|_{T'}\cdot\boldsymbol{n}_\mathfrak{f}\,\mu = 0\,.$$

Hence, $[\![\boldsymbol{\sigma}_h \cdot \boldsymbol{n}_{\mathfrak{f}}]\!]|_{\mathfrak{f}} = 0$ which implies that the normal component is continuous at the interelement boundaries, i.e., we have $\boldsymbol{\sigma}_h \in H(\mathrm{div},\Omega)$. □

Henceforth, to avoid technical diversions, we will also assume that $A|_T$ is a polynomial (its degree is irrelevant).

Proposition 4.2. *The recovered flux $\boldsymbol{\sigma}_h$ defined in* (4.9) *satisfies*

$$\int_K \nabla\cdot\boldsymbol{\sigma}_h\, v = \int_K f\, v \qquad \text{for all } v \in V_h^\ell(K) \quad \text{and} \quad \ell \geq 0.$$

Proof. First, assume $\ell \geq 1$, and note that, for all $v \in V_h^\ell(K)$, using integration by parts,

$$\int_K \nabla\cdot\boldsymbol{\sigma}_h\, v = \sum_{T\in\mathscr{T}_h^K}\int_T \nabla\cdot\boldsymbol{\sigma}_h\, v = \sum_{T\in\mathscr{T}_h^K}\left[-\int_T \boldsymbol{\sigma}_h\cdot\nabla v + \sum_{\mathfrak{f}\in\partial T}\int_{\mathfrak{f}} \boldsymbol{\sigma}_h\cdot\boldsymbol{n}_{\mathfrak{f}}\, v\right].$$

Since $\nabla v|_T \in \mathbb{P}_{\ell-1}(T)^d$, we can use (4.9) to get

$$\int_K \nabla\cdot\boldsymbol{\sigma}_h\, v = \sum_{T\in\mathscr{T}_h^K}\left[\int_T A\nabla u_{Hh}\cdot\nabla v - \sum_{\mathfrak{f}\in\partial T\cap\partial K}\int_{\mathfrak{f}}\lambda_H\, v\right] - \sum_{\mathfrak{f}\in\mathcal{F}_0^K\cap\mathcal{F}_T}\int_{\mathfrak{f}}[\![\{A\nabla u_{Hh}\}]\!]|_{\mathfrak{f}}\, v.$$

We know that $[\![\{A\nabla u_{Hh}\}]\!]|_{\mathfrak{f}} = 0$, then, using (3.11), $v = v_0 + v^\perp$, (3.8)-(3.9) and (3.10),

$$\begin{aligned}\int_K \nabla\cdot\boldsymbol{\sigma}_h\, v &= \sum_{T\in\mathscr{T}_h^K}\int_T A\nabla u_{Hh}\cdot\nabla v - \int_{\partial K}\lambda_H\, v \\ &= \sum_{T\in\mathscr{T}_h^K}\int_T A\nabla(T_h\lambda_H + \hat{T}_h f)\cdot\nabla v^\perp - \int_{\partial K}\lambda_H\, v = \int_K f\, v\,.\end{aligned}$$

For the case $\ell = 0$, we follow analogous steps, and get

$$\int_K \nabla\cdot\boldsymbol{\sigma}_h = \sum_{T\in\mathscr{T}_h^K}\int_T \nabla\cdot\boldsymbol{\sigma}_h = \sum_{T\in\mathscr{T}_h^K}\sum_{\mathfrak{f}\in\partial T}\int_{\mathfrak{f}}\boldsymbol{\sigma}_h\cdot\boldsymbol{n}_{\mathfrak{f}} = -\int_{\partial K}\lambda_H = \int_K f\,,$$

which finishes the proof. □

Let $\boldsymbol{\sigma} := -A\nabla u$. The next results shows the error estimate for $\nabla\cdot\boldsymbol{\sigma}_h$ in the $L^2(\Omega)-$norm.

Theorem 4.1. *Let $\ell \geq 0$ and $k \geq \ell + d$ be the polynomial orders of the MHM method* (3.10). *Assume that the exact solution of* (2.1) *satisfies $f \in H^{\ell+1}(\mathscr{P})$. Then the approximated flux $\boldsymbol{\sigma}_h \in H(div,\Omega)$ defined in* (4.9) *satisfies*

$$\|\nabla\cdot\boldsymbol{\sigma} - \Pi_{\Omega,\ell}(\nabla\cdot\boldsymbol{\sigma}_h)\|_{0,\Omega} \leq Ch^{\ell+1}|f|_{\ell+1,\mathscr{P}}\,.$$

Proof. It is not difficult to realize that Proposition 4.2 implies that $\Pi_{\Omega,\ell}(\nabla\cdot\boldsymbol{\sigma}_h) = \Pi_{\Omega,\ell}(\nabla\cdot\boldsymbol{\sigma}) = \Pi_{\Omega,\ell}(f)$. Then, using standard finite element approximation results (e.g. [19]) the following holds,

$$\|\nabla\cdot\boldsymbol{\sigma} - \Pi_{\Omega,\ell}(\nabla\cdot\boldsymbol{\sigma}_h)\|_{0,\Omega} = \|f - \Pi_{\Omega,\ell}(f)\|_{0,\Omega} \leq Ch^{\ell+1}|f|_{\ell+1,\mathscr{P}}\,,$$

which finishes the proof. □

The upcoming lemma holds significance about the error estimates for the post-processed dual variable.

Lemma 4.1. *Let $\mu \in \Lambda_H$. Then*

$$\|\mu\|_\star \leq C\,\|\mu\|_\Lambda\,. \tag{4.10}$$

Proof. Note that, for $\mu \in \Lambda_H$, there exists $\tilde{\boldsymbol{\tau}}_H \in \mathcal{RT}_\ell(\Xi_H)$ such that $\tilde{\boldsymbol{\tau}}_H \cdot \boldsymbol{n}^K = \mu$ on every $F \in \mathcal{E}_H$. Thus, using a local trace and inverse inequalities (c.f. [19, Lemma 12.8]), for a constant C independent of H, h and $\mathcal{H}$,

$$\|\mu\|_\star^2 = \sum_{K\in\mathscr{P}} \mathcal{H}_K \|\tilde{\boldsymbol{\tau}}_H \cdot \boldsymbol{n}^K\|_{0,\partial K}^2 \leq C \sum_{K\in\mathscr{P}} \|\tilde{\boldsymbol{\tau}}_H\|_{0,K}^2 \leq C \|\tilde{\boldsymbol{\tau}}_H\|_{\mathrm{div},\Omega}^2 \leq C \|\mu\|_\Lambda^2 ,$$

where we used the fact that $\boldsymbol{n}^K$ is the unit outward normal to ∂K, (2.5), and (2.4). □

The next result is an error estimate for the $L^2(\Omega)-$norm of $\boldsymbol{\sigma}_h$.

Theorem 4.2. *Let $\ell \geq 0$ and $k \geq \ell + d$ be the polynomial orders of the MHM method* (3.10)*. Assume that the exact solution of* (2.1) *satisfies $u \in H^{k+1}(\mathscr{P})$, $A\nabla u \in H^{\ell+1}(\mathscr{P}) \cap H(div,\Omega)$. Then the approximated flux $\boldsymbol{\sigma}_h \in H(div,\Omega)$ defined in* (4.9) *satisfies*

$$\|\boldsymbol{\sigma} - \boldsymbol{\sigma}_h\|_{0,\Omega} \leq C \left(h^k |u|_{k+1,\mathscr{P}} + H^{\ell+1} |A\nabla u|_{\ell+1,\mathscr{P}} \right) .$$

Proof. The triangle inequality gives,

$$\|\boldsymbol{\sigma} - \boldsymbol{\sigma}_h\|_{0,\Omega} \leq \underbrace{\left\{ \sum_{K\in\mathscr{P}} \|\boldsymbol{\sigma} - \pi_K^{\mathcal{RT}_\ell}\boldsymbol{\sigma}\|_{0,K}^2 \right\}^{1/2}}_{(i)} + \underbrace{\left\{ \sum_{K\in\mathscr{P}} \|\pi_K^{\mathcal{RT}_\ell}\boldsymbol{\sigma} - \boldsymbol{\sigma}_h\|_{0,K}^2 \right\}^{1/2}}_{(ii)} .$$

For (i), from (4.5), we have that

$$\left\{ \sum_{K\in\mathscr{P}} \|\boldsymbol{\sigma} - \pi_K^{\mathcal{RT}_\ell}\boldsymbol{\sigma}\|_{0,K}^2 \right\}^{1/2} \leq C H^{\ell+1} |A\nabla u|_{\ell+1,\mathscr{P}} . \tag{4.11}$$

Now we need to estimate (ii). We shall apply now (4.8) to $\boldsymbol{v}_h := (\pi_K^{\mathcal{RT}_\ell}\boldsymbol{\sigma} - \boldsymbol{\sigma}_h)|_T \in \mathcal{RT}_\ell(T)$. For all $T \in \mathscr{T}_h^K$ and $\boldsymbol{v}_h \in \mathcal{RT}_\ell(T)$,

$$\begin{aligned} \sum_{T\in\mathscr{T}_h^K} \|\boldsymbol{v}_h\|_{0,T}^2 \leq\ & C \sum_{T\in\mathscr{T}_h^K} \Big(\|\boldsymbol{\Pi}_{T,\ell-1}(\boldsymbol{v}_h)\|_{0,T}^2 + \\ & h_T \left\{ \sum_{\mathfrak{f}\subset\partial T\cap\partial K} \|\boldsymbol{v}_h \cdot \boldsymbol{n}_\mathfrak{f}\|_{0,\mathfrak{f}}^2 + \sum_{\mathfrak{f}\subset\mathcal{F}_0^K\cap\mathcal{F}_T} \|\boldsymbol{v}_h \cdot \boldsymbol{n}_\mathfrak{f}\|_{0,\mathfrak{f}}^2 \right\} \Big) \\ =\ & C \sum_{T\in\mathscr{T}_h^K} \big((a) + h_T\{(b)+(c)\} \big) . \end{aligned} \tag{4.12}$$

Let $T \in \mathscr{T}_h^K$, and let us bound (a). For $\boldsymbol{\tau} \in \mathbb{P}_{\ell-1}(T)^d$, using $\boldsymbol{\sigma} = -A\nabla u$ and the third equation in (4.9),

$$\int_T \boldsymbol{\Pi}_{T,\ell-1}(\boldsymbol{v}_h) \cdot \boldsymbol{\tau} = \int_T (\pi_T^{\mathcal{RT}_\ell}\boldsymbol{\sigma} - \boldsymbol{\sigma}_h) \cdot \boldsymbol{\tau} = \int_T A\nabla(u_{Hh} - u) \cdot \boldsymbol{\tau} .$$

Taking $\boldsymbol{\tau} = \boldsymbol{\Pi}_{T,\ell-1}(\boldsymbol{v}_h)$ and using the Cauchy-Schwarz inequality, we get

$$(a) = \|\boldsymbol{\Pi}_{T,\ell-1}(\boldsymbol{v}_h)\|_{0,T}^2 \leq \|A\nabla(u_{Hh} - u)\|_{0,T} \|\boldsymbol{\Pi}_{T,\ell-1}(\boldsymbol{v}_h)\|_{0,T} ,$$

which implies that

$$\|\boldsymbol{\Pi}_{T,\ell-1}(\boldsymbol{v}_h)\|_{0,T} \leq \|A\nabla(u_{Hh} - u)\|_{0,T} . \tag{4.13}$$

Now we only need to find estimates for (b) and (c). For (c), if $\mathfrak{f} \in \mathcal{F}_0^K \cap \mathcal{F}_T$, for all $\mu \in \mathbb{P}_\ell(\mathfrak{f})$, then from the definition of $\boldsymbol{\sigma}$, (4.9), (2.7) and (2.6), we get

$$\begin{aligned}\int_{\mathfrak{f}} \boldsymbol{v}_h \cdot \boldsymbol{n}_{\mathfrak{f}}\, \mu &= \int_{\mathfrak{f}} \pi_T^{\mathcal{RT}_\ell} \boldsymbol{\sigma} \cdot \boldsymbol{n}_{\mathfrak{f}}\, \mu + \int_{\mathfrak{f}} \{A\nabla u_{Hh}\} \cdot \boldsymbol{n}_{\mathfrak{f}}\, \mu \\ &= \int_{\mathfrak{f}} \pi_T^{\mathcal{RT}_\ell} \boldsymbol{\sigma} \cdot \boldsymbol{n}_{\mathfrak{f}}\, \mu + \int_{\mathfrak{f}} \frac{1}{2}(A\nabla u_{Hh}|_T + A\nabla u_{Hh}|_{T'}) \cdot \boldsymbol{n}_{\mathfrak{f}}\, \mu \\ &= \int_{\mathfrak{f}} \left(A\nabla u_{Hh}|_{T'} + \pi_T^{\mathcal{RT}_\ell} \boldsymbol{\sigma} + \frac{1}{2}[\![A\nabla u_{Hh}]\!] \right) \cdot \boldsymbol{n}_{\mathfrak{f}}\, \mu\,.\end{aligned}$$

Then, taking $\mu = \boldsymbol{v}_h \cdot \boldsymbol{n}_{\mathfrak{f}}$, from the Cauchy-Schwarz inequality,

$$(c) = \|\boldsymbol{v}_h \cdot \boldsymbol{n}_{\mathfrak{f}}\|_{0,\mathfrak{f}}^2 \leq C \|(A\nabla u_{Hh} + \pi_T^{\mathcal{RT}_\ell} \boldsymbol{\sigma} + [\![A\nabla u_{Hh}]\!]) \cdot \boldsymbol{n}_{\mathfrak{f}}\|_{0,\mathfrak{f}} \|\boldsymbol{v}_h \cdot \boldsymbol{n}_{\mathfrak{f}}\|_{0,\mathfrak{f}}\,,$$

and, from Theorem A.2,

$$\|(A\nabla u_{Hh} + \pi_T^{\mathcal{RT}_\ell} \boldsymbol{\sigma} + [\![A\nabla u_{Hh}]\!]) \cdot \boldsymbol{n}_{\mathfrak{f}}\|_{0,\mathfrak{f}} \leq C_A \sum_{T' \in \omega_{\mathfrak{f}}} h_T^{-1/2} |u - u_{Hh}|_{1,T'}\,.$$

Summing up over all internal facets implies that,

$$\left\{ \sum_{\mathfrak{f} \subset \mathcal{F}_0^K \cap \mathcal{F}_T} \|\boldsymbol{v}_h \cdot \boldsymbol{n}_{\mathfrak{f}}\|_{0,\mathfrak{f}}^2 \right\}^{1/2} \leq C_A \sum_{\mathfrak{f} \in \mathcal{F}_0^K \cap \mathcal{F}_T} \sum_{T' \in \omega_{\mathfrak{f}}} h_T^{-1} |u - u_{Hh}|_{1,T'}^2\,. \tag{4.14}$$

On the other hand, for (b), if $\mathfrak{f} \subset \partial T \cap \partial K$ and $\lambda \in L^2(\partial K)$, for all $\mu \in \mathbb{P}_\ell(\mathfrak{f})$, from the first equation in (4.9) and the definition of $\Pi_{\mathcal{E},\ell}(\cdot)$, we get

$$\begin{aligned}\sum_{\mathfrak{f} \subset \partial T \cap \partial K} \int_{\mathfrak{f}} \boldsymbol{v}_h \cdot \boldsymbol{n}_{\mathfrak{f}}\, \mu &= \sum_{\mathfrak{f} \subset \partial T \cap \partial K} \int_{\mathfrak{f}} (\boldsymbol{\sigma} \cdot \boldsymbol{n}_{\mathfrak{f}} - \boldsymbol{\sigma}_h \cdot \boldsymbol{n}_{\mathfrak{f}})\mu \\ &= \int_{\partial K} (-\lambda + \lambda_H)\mu \\ &= \int_{\partial K} (-\Pi_{\mathcal{E},\ell}(\lambda) + \lambda_H)\mu\,.\end{aligned}$$

Again, taking $\mu = \boldsymbol{v}_h \cdot \boldsymbol{n}_{\mathfrak{f}}$, from the Cauchy-Schwarz inequality,

$$(b) = \sum_{\mathfrak{f} \subset \partial T \cap \partial K} \|\boldsymbol{v}_h \cdot \boldsymbol{n}_{\mathfrak{f}}\|_{0,\mathfrak{f}}^2 \leq \|\Pi_{\mathcal{E},\ell}(\lambda) - \lambda_H\|_{0,\partial K} \left\{ \sum_{\mathfrak{f} \subset \partial T \cap \partial K} \|\boldsymbol{v}_h \cdot \boldsymbol{n}_{\mathfrak{f}}\|_{0,\mathfrak{f}}^2 \right\}^{1/2},$$

which implies that

$$\left\{ \sum_{\mathfrak{f} \subset \partial T \cap \partial K} \|\boldsymbol{v}_h \cdot \boldsymbol{n}_{\mathfrak{f}}\|_{0,\mathfrak{f}}^2 \right\}^{1/2} \leq \|\Pi_{\mathcal{E},\ell}(\lambda) - \lambda_H\|_{0,\partial K}\,. \tag{4.15}$$

Then, applying (4.13)-(4.15) to (4.12) we obtain

$$\begin{aligned}\sum_{T \in \mathscr{T}_h^K} \|\boldsymbol{v}_h\|_{0,T}^2 &\leq C \Big[\sum_{T \in \mathscr{T}_h^K} \Big(\|A\nabla(u_{Hh} - u)\|_{0,T}^2 + h_T \|\Pi_{\mathcal{E},\ell}(\lambda) - \lambda_H\|_{0,\partial K}^2 \Big) \\ &\qquad + \sum_{\mathfrak{f} \in \mathcal{F}_0^K \cap \mathcal{F}_T} \sum_{T' \in \omega_{\mathfrak{f}}} \|A\nabla(u - u_{Hh})\|_{0,T}^2 \Big] \\ &\leq C \sum_{T \in \mathscr{T}_h^K} \Big(\|u - u_{Hh}\|_{1,T}^2 + h_T \|\Pi_{\mathcal{E},\ell}(\lambda) - \lambda_H\|_{0,\partial K}^2 \Big)\,.\end{aligned} \tag{4.16}$$

Finally, adding over $K \in \mathscr{P}$ and using (2.10) we get

$$\|\boldsymbol{v}_h\|_{0,\mathscr{P}} \leq C \left\| u - u_{Hh} \right\|_V + \|\Pi_{\mathcal{E},\ell}(\lambda) - \lambda_H\|_\star\,.$$

Now, we only need to find an estimate for $\|\Pi_{\mathcal{E},\ell}(\lambda) - \lambda_H\|_\star$. From (4.10) we have that

$$\|\Pi_{\mathcal{E},\ell}(\lambda) - \lambda_H\|_\star \leq C\,\|\Pi_{\mathcal{E},\ell}(\lambda) - \lambda_H\|_\Lambda \leq C\,\left(\|\Pi_{\mathcal{E},\ell}(\lambda) - \lambda\|_\Lambda + \|\lambda - \lambda_H\|_\Lambda\right)\,,$$

where we used the fact that $\Pi_{\mathcal{E},\ell}(\lambda) \in \Lambda_H$ and $\lambda_H \in \Lambda_H$. Then, from Theorem 3.1 and global interpolation (c.f. [19, Section 19.3]),

$$\|\lambda - \lambda_H\|_\star \leq C(h^k|u|_{k+1,\mathscr{P}} + H^{\ell+1}|A\nabla u|_{\ell+1,\mathscr{P}})\,.$$

We then arrive that, the estimate for (ii) is,

$$\left\{\sum_{K\in\mathscr{P}} \|\pi_K^{\mathcal{RT}_\ell}\boldsymbol{\sigma} - \boldsymbol{\sigma}_h\|_{0,K}^2\right\}^{1/2} \leq C\,\left(h^k|u|_{k+1,\mathscr{P}} + H^{\ell+1}|A\nabla u|_{\ell+1,\mathscr{P}}\right)\,.$$

From (i) and (ii) we have

$$\|\boldsymbol{\sigma} - \boldsymbol{\sigma}_h\|_{0,\Omega} \leq C\,\left(h^k|u|_{k+1,\mathscr{P}} + H^{\ell+1}|A\nabla u|_{\ell+1,\mathscr{P}}\right)\,, \tag{4.17}$$

which finishes the proof. □

5. A fully computable *a posteriori* error bound

In this section, we propose and analyze a computable and efficient procedure for *a posteriori* error estimation for the provided approximate solutions. An *a posteriori* error estimation is fundamental for efficient error control of numerical simulations. The purpose is to use them to control the error and/or to adaptively modify the discretization to get the desired accuracy with reduced computational effort. Some properties are expected for an optimal *a posteriori* error estimator, namely, a guaranteed upper bound, i.e., the *a posteriori* estimator is fully computable from u_{Hh} and $\boldsymbol{\sigma}_h$, [10]. An *a posteriori* error estimate aims at giving bounds on the error between the known numerical approximation and the unknown exact solution that can be computed in practice, once the approximate solution is known [20].

To analyze the *a posteriori* estimator we need to impose the following extra conditions.

Assumption B: The union $\mathscr{T}_h := \cup_{K\in\mathscr{P}}\mathscr{T}_h^K$ forms a conforming triangulation of $\bar{\Omega}$.

Assumption C: For every $F \in \mathcal{E}_H$, and every $\mathfrak{f} \in \mathcal{F}_h^K \cap \partial K$ s.t. $\mathfrak{f} \subseteq F$ we have $H_F \leq C\,h_\mathfrak{f}$, where C does not depend on h, H or $\mathcal{H}$.

Assumption D: $\mathscr{P}$ consists of convex polytopes K.

Remark 5.1. *Assumption C states that the submesh $\mathscr{T}_h^K$ cannot be much finer than $\mathcal{E}_H$. As the leading error estimates for the method are given by $H^{\ell+1}$, this assumption is not really restrictive.*

Remark 5.2. *Assumption B, also allows us to modify the flux recovery $\boldsymbol{\sigma}_h$ slightly. In fact, since the union of the local triangulations $\mathscr{T}_h^K$ defines a conforming triangulation in the whole domain, we can modify the definition of $\boldsymbol{\sigma}_h$ in the following way: For $\ell \leq m \leq k$, $\boldsymbol{\sigma}_h \in \mathcal{RT}_m(T)$ is defined as, with*

$k \geq \ell + d$

(5.1)
$$\begin{cases} \displaystyle\int_{\mathfrak{f}} (\boldsymbol{\sigma}_h \cdot \boldsymbol{n}_{\mathfrak{f}})\mu = \int_{\mathfrak{f}} -\lambda_H\,\mu & \text{for all } \mu \in \mathbb{P}_m(\mathfrak{f}),\ \text{if } \mathfrak{f} \subset \partial K \cap \partial T\,, \\ \displaystyle\int_{\mathfrak{f}} (\boldsymbol{\sigma}_h \cdot \boldsymbol{n}_{\mathfrak{f}})\mu = \int_{\mathfrak{f}} -\{A\nabla u_{Hh}\}\cdot\boldsymbol{n}_{\mathfrak{f}}\,\mu & \text{for all } \mu \in \mathbb{P}_m(\mathfrak{f}),\ \text{if } \mathfrak{f} \in \mathcal{F}_0^K \cap \mathcal{F}_T\,, \\ \displaystyle\int_T \boldsymbol{\sigma}_h \cdot \boldsymbol{\tau} = \int_T -A\nabla u_{Hh}\cdot\boldsymbol{\tau} & \text{for all } \boldsymbol{\tau} \in \mathbb{P}_{m-1}(T)^d,\ (m \geq 1)\,. \end{cases}$$

This definition extends (4.9) *allowing us to recover the flux* $\boldsymbol{\sigma}_h$ *onto a higher-order polynomial degree. Theorems 4.2 and 4.1 also apply, and we can, in particular, prove*

$$\|\nabla\cdot\boldsymbol{\sigma} - \Pi_{\Omega,m}(\nabla\cdot\boldsymbol{\sigma}_h)\|_{0,\Omega} \leq Ch^{m+1}|f|_{m+1,\mathscr{P}}\,,$$

where $C > 0$ *is a constant independent of* h.

Now we introduce the Oswald interpolation operator $I_{OS} : V_h^k \to V_h^k \cap H_0^1(\Omega)$ [34, 22] as follows: for $\varphi_h \in V_h^k$ and a Lagrange node $V \in \Omega$,

$$I_{OS}(\varphi_h)(V) = \frac{1}{\#\widehat{\mathscr{T}_V}} \sum_{T\in\widehat{\mathscr{T}_V}} \varphi_h|_T(V)\,, \tag{5.2}$$

where $\widehat{\mathscr{T}_V} := \{T \in \mathscr{T}_h \,:\, V \in T\}$ and $\#\widehat{\mathscr{T}_V}$ denotes the cardinality of the set $\widehat{\mathscr{T}_V}$.

With these ingredients, we present the main result in *a posteriori* estimator.

Theorem 5.1. *Assume* $\ell \geq 0$, $k \geq \ell + d$ *and* $\ell \leq m \leq k$. *Let* $u \in H_0^1(\Omega)$ *be the solution of* (2.1), *and* u_{Hh} *be the solution of the MHM method* (3.10). *Let* $\boldsymbol{\sigma}_h$ *be the equilibrated flux reconstruction defined through* (5.1), *and defined the local quantities*

$$\eta_{1,K} := \|A\nabla\, u_{Hh} + \boldsymbol{\sigma}_h\|_{0,K}\,, \tag{5.3}$$

and

$$\eta_{2,K} = \|A\nabla(u_{Hh} - I_{OS}(u_{Hh}))\|_{0,K}\,. \tag{5.4}$$

Then, the following upper bound holds

$$\|A\nabla(u - u_{Hh})\|_{0,\mathscr{P}}^2 \leq \eta^2 := \sum_{K\in\mathscr{P}} (\eta_{1,K} + \eta_{osc,K}^f)^2 + \sum_{K\in\mathscr{P}} \eta_{2,K}^2\,, \tag{5.5}$$

where for any $K \in \mathscr{P}$ *convex,* $\eta_{osc,K}^f$ *is the oscillation term defined by*

$$\eta_{osc,K}^f := \frac{\mathcal{H}_K}{\pi}\|f - \Pi_{K,m}(f)\|_{0,K}\,. \tag{5.6}$$

In addition, assuming $\boldsymbol{\sigma} := -A\nabla u \in H(div,\Omega)\cap H^s(\Omega)$, $s > 1/2$, *the following local lower bounds hold*

$$\begin{aligned} &\eta_{1,K} \leq C\,\|A\nabla(u - u_{Hh})\|_{0,K} + \eta_{osc,K}^{\boldsymbol{\sigma}} + H^{1/2}\|\Pi_{\mathcal{E},m}(\lambda) - \lambda_H\|_{0,\partial K}\,, \\ &\eta_{2,K} \leq C\|A\nabla(u - u_{Hh})\|_{0,\omega_K}\,, \end{aligned} \tag{5.7}$$

where is the oscillation term

$$\eta_{osc,K}^{\boldsymbol{\sigma}} := \|\boldsymbol{\sigma} - \pi_K^{\mathcal{RT}_m}\boldsymbol{\sigma}\|_{0,K}\,, \tag{5.8}$$

and $\omega_K := \{\kappa \in \Xi_H^K \,:\, \kappa \subset K \quad or \quad \kappa \cap K = F \in \mathcal{E}_H\}$.

Moreover, the following global lower bound holds

$$\eta^2 \leq \Big(\|A\nabla(u_{Hh} - u)\|_{0,\mathscr{P}}^2 + \|\Pi_{\mathcal{E},m}(\lambda) - \lambda_H\|_\Lambda^2 + \sum_{K\in\mathscr{P}} (\eta_{osc,K}^{\boldsymbol{\sigma}})^2\Big). \tag{5.9}$$

Remark 5.3. *It is important to mention that, since we allow* $m \geq \ell$, *then* $\eta_{osc,K}^{\boldsymbol{\sigma}}$ *and* $\eta_{osc,K}^f$ *are indeed oscillations for* $m > \ell$.

Remark 5.4. *In the case where $K \in \mathscr{P}$ is not convex, we can still propose an estimator, but not a fully computable one where* (5.6) *can be written as*

$$\eta^f_{osc,K} := C_P\, \mathcal{H}_K \|f - \Pi_{K,m}(f)\|_{0,K}\,,$$

and $C_P > 0$ is a constant independent of K according to the Poincaré-Wirtinger inequality, which proof can be found in [36, Theorem 3.2].

Proof. Let $s \in H^1_0(\Omega)$ be the unique solution of

$$(\nabla s, \nabla v)_{\mathscr{P}} = (\nabla u_{Hh}, \nabla v)_{\mathscr{P}} \quad \forall\, v \in H^1_0(\Omega)\,. \tag{5.10}$$

Then from the Pythagorean equality

$$\|A\nabla(u - u_{Hh})\|^2_{0,\Omega} = \|A\nabla(u - s)\|^2_{0,\mathscr{P}} + \|A\nabla(s - u_{Hh})\|^2_{0,\mathscr{P}}\,. \tag{5.11}$$

Moreover,

$$\|A\nabla(s - u_{Hh})\|^2_{0,\mathscr{P}} = \min_{w \in H^1_0(\Omega)} \|A\nabla(w - u_{Hh})\|^2_{0,\mathscr{P}}\,. \tag{5.12}$$

It follows from (5.12) that, for $w = I_{OS}(u_{Hh})$, we have the bound

$$\|A\nabla(s - u_{Hh})\|^2_{0,\mathscr{P}} \le \|A\nabla(u_{Hh} - I_{OS}(u_{Hh}))\|^2_{0,\mathscr{P}} = \sum_{K\in\mathscr{P}} \eta^2_{2,K}\,. \tag{5.13}$$

For the first term in (5.11), we note that $u - s \in H^1_0(\Omega)$. Thus, from the definition of $s \in H^1_0(\Omega)$ and the energy norm for a function in $H^1_0(\Omega)$,

$$\|A\nabla(u - s)\|^2_{0,\Omega} = \sup_{\substack{\varphi\in H^1_0(\Omega)\\ |\varphi|_{1,\Omega}=1}} (A\nabla(u - s), \nabla\varphi)_{\mathscr{P}} = \sup_{\substack{\varphi\in H^1_0(\Omega)\\ |\varphi|_{1,\Omega}=1}} (A\nabla(u - u_{Hh}), \nabla\varphi)_{\mathscr{P}}\,,$$

where we used that (5.10) implies $(A\nabla(s - u_{Hh}), \nabla\varphi)_{\mathscr{P}} = 0$. Let now $\varphi \in H^1_0(\Omega)$ with $|\varphi|_{1,\Omega} = 1$ be fixed. Using the weak formulation (2.1), adding and subtracting $(\boldsymbol{\sigma}_h, \nabla\varphi)_{\mathscr{P}}$, $\boldsymbol{\sigma}_h \in H(\mathrm{div}, \Omega)$ defined in (5.1) and integration by parts, we have

$$\begin{aligned}(A\nabla(u - u_{Hh}), \nabla\varphi)_{\mathscr{P}} &= (A\nabla u, \nabla\varphi)_{\mathscr{P}} - (A\nabla u_{Hh}, \nabla\varphi)_{\mathscr{P}}\\ &= (f - \nabla\cdot\boldsymbol{\sigma}_h, \varphi)_{\mathscr{P}} - (A\nabla u_{Hh} + \boldsymbol{\sigma}_h, \nabla\varphi)_{\mathscr{P}}\,.\end{aligned}$$

The Cauchy-Schwarz inequality gives

$$-(A\nabla u_{Hh} + \boldsymbol{\sigma}_h, \nabla\varphi)_{\mathscr{P}} \le \sum_{K\in\mathscr{P}} \|A\nabla u_{Hh} + \boldsymbol{\sigma}_h\|_{0,K}\|\nabla\varphi\|_{0,K} = \sum_{K\in\mathscr{P}} \eta_{1,K}\|\nabla\varphi\|_{0,K}\,,$$

and from Proposition 4.2, the Poincaré inequality and Cauchy-Schwarz inequality,

$$\begin{aligned}(f - \nabla\cdot\boldsymbol{\sigma}_h, \varphi)_{\mathscr{P}} &= \sum_{K\in\mathscr{P}} (f, \varphi)_K - (\nabla\cdot\boldsymbol{\sigma}_h, \varphi)_K\\ &= \sum_{K\in\mathscr{P}} (f, \varphi)_K - (\nabla\cdot\boldsymbol{\sigma}_h, \Pi_{K,m}(\varphi))_K\\ &= \sum_{K\in\mathscr{P}} (f - \Pi_{K,m}(f), \varphi - \overline{\varphi}_K)_K\\ &\le \sum_{K\in\mathscr{P}} \frac{\mathcal{H}_K}{\pi}\|f - \Pi_{K,m}(f)\|_{0,K}\|\nabla\varphi\|_{0,K} = \sum_{K\in\mathscr{P}} \eta^f_{\mathrm{osc},K}\|\nabla\varphi\|_{0,K}\,,\end{aligned}$$

where $\overline{\varphi}_K := (\varphi, 1)/|K|$ and $\Pi_{K,m}(\cdot)$ is defined in (3.5). Combining the above results we get to

$$\|A\nabla(u-s)\|^2_{0,\Omega} \le \left(\sup_{\substack{\varphi\in H^1_0(\Omega)\\ |\varphi|_{1,\Omega}=1}} \sum_{K\in\mathscr{P}} (\eta_{1,K} + \eta^f_{\mathrm{osc},K})\|\nabla\varphi\|_{0,K}\right)^2 \le \sum_{K\in\mathscr{P}} (\eta_{1,K} + \eta^f_{\mathrm{osc},K})^2\,. \tag{5.14}$$

Therefore, from (5.13) and (5.14),

$$\|A\nabla(u-u_{Hh})\|_{0,\mathscr{P}} \leq \left\{ \sum_{K\in\mathscr{P}} (\eta_{1,K}+\eta^f_{\mathrm{osc},K})^2 + \sum_{K\in\mathscr{P}} \eta^2_{2,K} \right\}^{1/2}.$$

Now, for the lower bound, from [11, 29] and Assumption C, it follows that

$$\begin{aligned}\eta_{2,K} = \|A\nabla(u_{Hh}-I_{OS}(u_{Hh}))\|_{0,K} &\leq C \left\{ \sum_{\mathfrak{f}\in\mathcal{F}_h^K} h_{\mathfrak{f}}^{-1}\|[\![u_{Hh}]\!]\|^2_{0,\mathfrak{f}} \right\}^{1/2} \\ &\leq C\,C_0 \left\{ \sum_{F\in\mathcal{E}_H} H_F^{-1}\|[\![u_{Hh}]\!]\|^2_{0,F} \right\}^{1/2}.\end{aligned}$$

Let $F\in\mathcal{E}_H$, using $\mu\in\Lambda_H$ given by $\mu=1$ in F and $\mu=0$ elsewhere, in the second equation of the MHM method (3.10) we get $\langle [\![u_{Hh}]\!], 1\rangle_F = 0$. So, applying [2, Theorem 10] we get

$$H_F^{-1}\|[\![u_{Hh}]\!]\|^2_{0,F} \leq C\,\|A\nabla(u-u_{Hh})\|^2_{0,\tilde{\omega}_F},$$

where $\tilde{\omega}_F = \kappa_F\cup\tilde{\kappa}_F$, $\kappa_F\subseteq K$ and $\tilde{\kappa}_F\subseteq K'$. For all $K\in\mathscr{P}$,

$$\left\{ \sum_{F\in\mathcal{E}_H\cap\partial K} H_F^{-1}\|[\![u_{Hh}]\!]\|^2_{0,F} \right\}^{1/2} \leq C\|A\nabla(u-u_{Hh})\|_{0,\omega_K}.$$

Therefore,

$$\eta_{2,K} = \|A\nabla(u_{Hh}-I_{OS}(u_{Hh}))\|_{0,K} \leq C\|A\nabla(u-u_{Hh})\|_{0,\omega_K}.$$

To bound $\eta_{1,K}$ we notice that, since $\boldsymbol{\sigma} = -A\nabla u \in H(\mathrm{div},\Omega)\cap H^s(\Omega)^d$, $s>1/2$, then $\lambda\in L^2(\mathcal{E})$, so using the triangle inequality and (4.16) we get

$$\begin{aligned}\eta_{1,K} &= \|A\nabla u_{Hh}+\boldsymbol{\sigma}_h\|_{0,K} \\ &\leq \|A\nabla u_{Hh}-\boldsymbol{\sigma}\|_{0,K} + \|\boldsymbol{\sigma}-\pi_K^{\mathcal{RT}_m}\boldsymbol{\sigma}\|_{0,K} + \|\pi_K^{\mathcal{RT}_m}\boldsymbol{\sigma}-\boldsymbol{\sigma}_h\|_{0,K} \\ &\leq \|A\nabla(u_{Hh}-u)\|_{0,K} + \|\boldsymbol{\sigma}-\pi_K^{\mathcal{RT}_m}\boldsymbol{\sigma}\|_{0,K} + \|\pi_K^{\mathcal{RT}_m}\boldsymbol{\sigma}-\boldsymbol{\sigma}_h\|_{0,K} \\ &\leq C\,\|A\nabla(u-u_{Hh})\|_{0,K} + \eta^{\boldsymbol{\sigma}}_{\mathrm{osc},K} + H^{1/2}\|\Pi_{\mathcal{E},m}(\lambda)-\lambda_H\|_{0,\partial K}.\end{aligned}$$

Finally, adding in $K\in\mathscr{P}$, we get (5.9) which finishes the proof.

□

6. Numerical Results

This section verifies the theoretical aspects of this work. The following numerical results are based on an implementation using FreeFem++ [27]. Since one of the objectives is to validate the *a posteriori* error estimates, we build $\boldsymbol{\sigma}_h$ using $\ell\leq m\leq k$ with $k\geq\ell+d$ defined in (5.1) on conforming meshes. The expected orders of convergence are given by Table 1.

Error estimates	**Order**
$\|u-u_{Hh}\|_{1,\Omega}$	$h^k+H^{\ell+1}$
$\|\boldsymbol{\sigma}-\boldsymbol{\sigma}_h\|_{0,\Omega}$	$h^k+H^{\ell+1}$
$\|\nabla\cdot\boldsymbol{\sigma}-\Pi_{\Omega,m}(\nabla\cdot\boldsymbol{\sigma}_h)\|_{0,\Omega}$	h^{m+1}

Table 1. Error estimates order for $\ell\geq 0$, $k\geq\ell+d$ and $\ell\leq m\leq k$.

6.1. **A smooth case with an analytical solution.** The goal of this experiment is to assess the theoretical results using a smooth analytical solution. We consider $A = Id$, and the right-hand side and boundary conditions are chosen such that

$$u(x, y) = \sin(2\pi x)\sin(2\pi y)\,,$$

solves (2.1). Here we are using a conforming mesh where both global and local meshes are based on triangles.

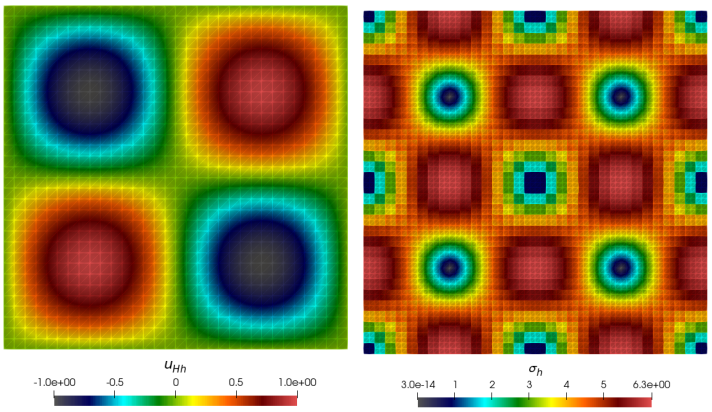

FIGURE 2. The solution u_{Hh} (left) and $\boldsymbol{\sigma}_h$ from the flux recovery strategy (right).

Figure 2 shows the approximate solution, u_{Hh}, computed through the MHM method (3.10) using $\ell = 0$ and $k = 2$ and the approximate flux $\boldsymbol{\sigma}_h$ built using the flux recovery strategy in (5.1) for $m = 2$.

The convergence results in the $L^2(\Omega)-$norm for the flux variable $\boldsymbol{\sigma}_h$ using the solution of the MHM method with $\ell \in \{0, 1\}$ and $k \in \{2, 3\}$ in a conforming mesh are depicted in Figure 3.

We observe a convergence which is consistent with the theoretical error estimates. In fact, the theoretical results predict that the $L^2(\Omega)-$norm for the flux, as derived from the recovery strategy, exhibit a convergence rate of $\mathcal{O}(H^{\ell+1})$. Furthermore, according to Remark 5.2, we can also see in Figure 3 that using $\ell \leq m \leq k$ for a conforming mesh, the divergence of $\boldsymbol{\sigma}_h$ converges at rate $\mathcal{O}(h^{m+1})$.

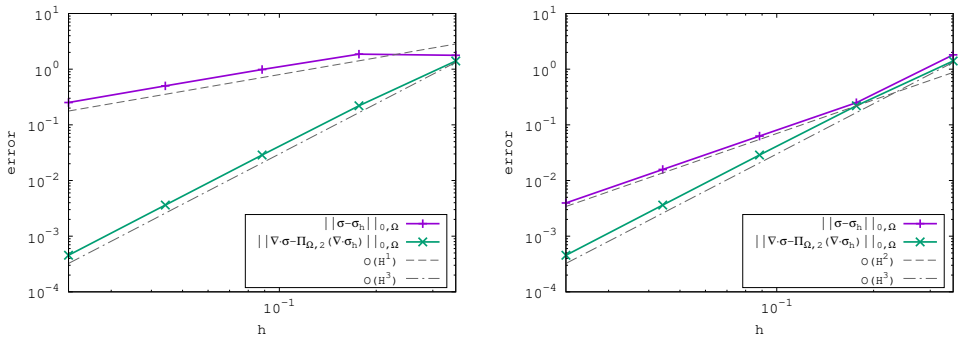

FIGURE 3. The convergence on simplicial elements in the $L^2(\Omega)-$norm for $\ell = 0$ (left) and $\ell = 1$(right) and $\boldsymbol{\sigma}_h$ with $m = 2$. Here $h = \frac{\mathcal{H}}{2}$ and $k = \ell + 2$.

Figure 4 shows a comparison between the divergence of the flux obtained through simple post-processing of the primal variable, namely, $-\nabla \cdot A\nabla u_{Hh}$, and the flux obtained from (5.1), with $\ell = 0$, $k = 2$ and $m = 2$. It is interesting to note that $\boldsymbol{\sigma}_h$ from our proposed strategy converges with the optimal order of $\mathcal{O}(h^{m+1})$ in the $L^2(\Omega)-$norm while the other approach does not converge.

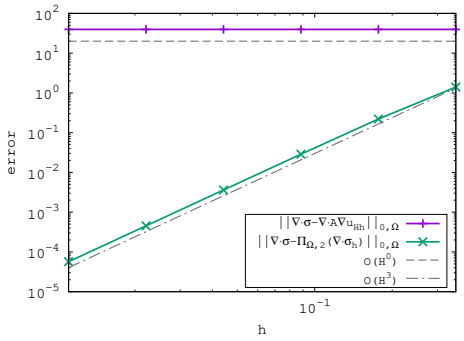

FIGURE 4. The convergence on simplicial elements for the $L^2(\Omega)-$norm for $\ell = 0$, $k = 2$ and $m = 2$. Here $h = \frac{\mathcal{H}}{2}$.

Now, regarding the *a posteriori* estimator defined in Section 5, Tables 2 and 3 report the error in the energy norm $\|A\nabla(u - u_{Hh})\|_{0,\mathscr{P}}$, the global estimator η as well as the individual estimators $\eta_1 := \|A\nabla u_{Hh} + \boldsymbol{\sigma}_h\|_{0,\mathscr{P}}$, $\eta_2 := \|A\nabla(u_{Hh} - I_{OS}(u_{Hh}))\|_{0,\mathscr{P}}$, and the data oscillations η^f_{osc} and $\eta^{\boldsymbol{\sigma}}_{osc}$ for the MHM solution with $\ell = \{0, 1\}$ and $k = \{2, 3\}$, and for the flux recovery strategy with $m = 2$. We can observe that η^f_{osc} and $\eta^{\boldsymbol{\sigma}}_{osc}$ are indeed oscillations and the estimator get tighter.

Tables 2 and 3 also reports the effectivity indices (overestimation factor) defined as

$$I^{eff} := \frac{\eta}{\|A\nabla(u - u_{Hh})\|_{0,\mathscr{P}}},$$

and the corresponding orders of convergence (in parentheses).

h	ℓ	k	m	$\|A\nabla(u-u_{Hh})\|_{0,\mathscr{P}}$	η_1	η_2	η^f_{osc}	$\eta^{\boldsymbol{\sigma}}_{osc}$	η	I^{eff}
0.176	0	2	2	1.865	0.149	2.391	0.016	0.008	2.39	1.287
0.088				0.987 (0.91)	0.031 (2.25)	1.219 (0.97)	0.001 (3.91)	0.001 (3.06)	1.219 (0.97)	1.236
0.044				0.501 (0.97)	0.007 (2.09)	0.609 (1.00)	6.7e-05 (3.97)	1.2e-04 (3.01)	0.609 (1.00)	1.216
0.022				0.251 (0.99)	0.001 (2.02)	0.304 (1.00)	4.2e-06 (3.99)	1.5e-05 (3.00)	0.304 (1.00)	1.210
0.011				0.125 (0.99)	4.4e-04 (2.00)	0.152 (1.00)	2.6e-07 (3.99)	1.9e-06 (3.00)	0.152 (1.00)	1.208

TABLE 2. Numerical validation of the a posteriori error estimator η with $\ell = 0$ and $k = 2$.

h	ℓ	k	m	$\|A\nabla(u-u_{Hh})\|_{0,\mathscr{P}}$	η_1	η_2	η^f_{osc}	$\eta^{\boldsymbol{\sigma}}_{osc}$	η	I^{eff}
0.176	1	3	2	0.242	0.048	0.292	0.016	0.008	0.297	1.223
0.088				0.060 (1.99)	0.012 (1.98)	0.074 (1.97)	0.001 (3.91)	0.001 (3.06)	0.075 (1.97)	1.236
0.044				0.015 (1.99)	0.003 (1.99)	0.018 (1.98)	6.7e-05 (3.97)	1.2e-04 (3.01)	0.018 (1.98)	1.242
0.022				0.003 (1.99)	7.7e-04 (2.00)	0.004 (1.99)	4.2e-06 (3.99)	1.5e-05 (3.00)	0.004 (1.99)	1.244
0.011				9.5e-04 (1.99)	1.9e-04 (2.00)	0.001 (1.99)	2.6e-07 (3.99)	1.92e-06 (3.00)	0.001 (1.99)	1.245

TABLE 3. Numerical validation of the a posteriori error estimator η with $\ell = 1$ and $k = 3$.

As predicted by the theory, the estimator η is a strict upper bound for the discretization error. The effectivity indices also show a robust behavior.

6.2. **SPE 10.** We use Model 2 of the 10th Society of Petroleum Engineers Comparative Solution Project (c.f. [14]) hereafter referred to as the SPE-10 model.

To validate our flux recovery strategy described in (5.1), we choose layer 36 as the object of our study and set the entry pressures as $u = 1$ (bottom) and exit $u = 0$ (top). On the other two boundaries, we set homogeneous Neumann conditions.

Since this benchmark does not have an analytical solution, we used a standard mixed formulation using Raviart-Thomas spaces of order 2 on a mesh of 125.000 triangular elements and 1.314.000 degrees of freedom to obtain a reference solution for this case.

Figure 5 shows that $|\boldsymbol{\sigma}_h|$ from the flux recovery strategy in (5.1) with $m = 2$ approximates the canal better than the current approximation done in the MHM method using $-\nabla \cdot A\nabla u_{Hh}$.

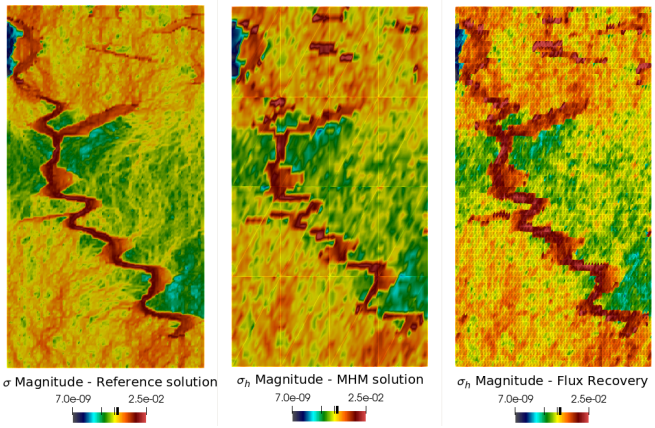

FIGURE 5. The reference solution (left). The dual variable obtained from $-A\nabla u_{Hh}$ (middle) and from the flux recovery strategy with $m = 2$ (right) using the MHM method with $\ell = 0$ and $k = 2$.

We next test the performance of the *a posteriori* estimator defined in (5.5). We start with a coarse initial mesh of 512 elements and 4 elements in the submesh and build an adaptive algorithm based on the remeshing routine in FreeFem++ (see [27, Section 5.1.9] for a complete description). In Figure 6 we depict a sequence of adapted meshes obtained with this strategy while in Figure 7 $|\boldsymbol{\sigma}_h|$ is depicted in the first and last meshes along with the reference solution. The last adapted mesh has 3.166 elements and 7.973 degrees of freedom.

Finally, in Figure 8 we depict a diagonal cross-section of u_{Hh} from $(0, 0)$ to $(1200, 2200)$ where we can observe the improvement induced by the use of adaptive meshes.

7. CONCLUSIONS

In this work, we have introduced a localized post-processing strategy designed to construct an approximate flux based on the solution derived from the MHM method. Also, as a byproduct of the flux recovery strategy, we introduced and analyzed an *a posteriori* estimator.

The main contribution is regarding how we deal with the flux recovery when we take into account face mesh partitions and second-level meshes in the MHM method. This is exactly the scenario when the MHM method is used to approximate the solution of multiscale problems. We proposed a new cheap, local system to post-process the dual variable and, following this, we conducted a convergence analysis. We proved that this approximation achieves

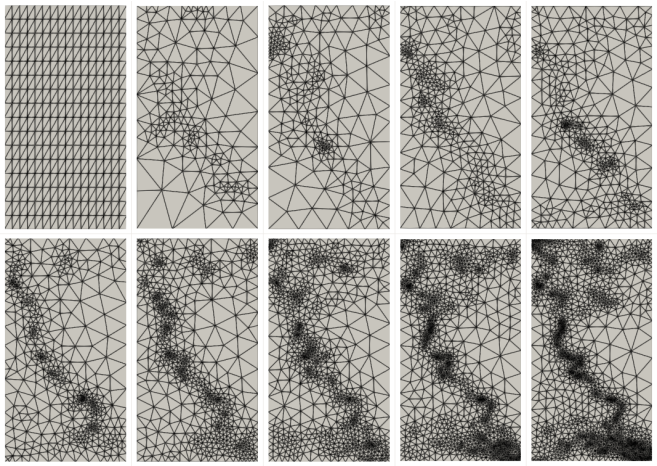

FIGURE 6. Sequence of adapted meshes induced by the *a posteriori* estimator η. Here $\ell = 0$.

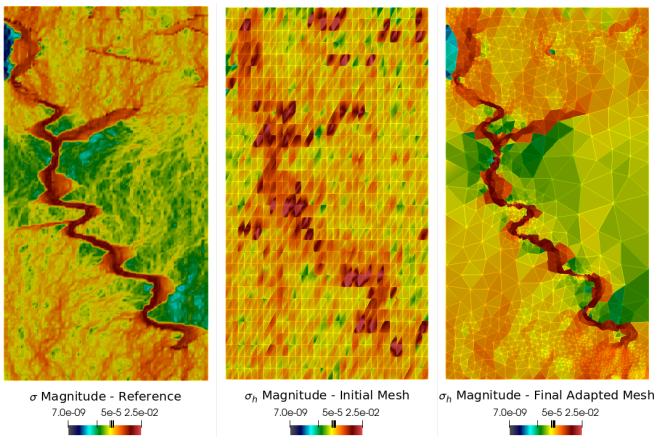

FIGURE 7. Isolines of $|\boldsymbol{\sigma}_h|$ obtained from the reference solution (left) and from the MHM method using the initial mesh (middle) and the adapt mesh (right).

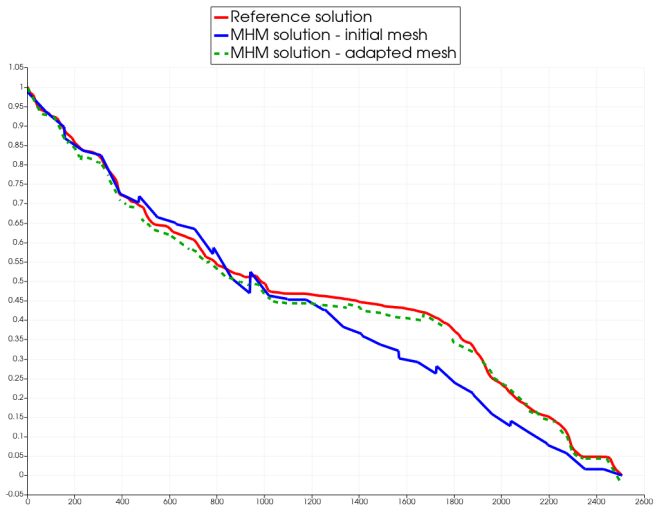

FIGURE 8. Comparison of the profile of the reference solution and the MHM's solution u_{Hh} obtained on the initial and final adapt meshes. Here $\ell = 0$.

optimal convergence orders of $\mathcal{O}(H^{\ell+1})$ in the $L^2(\Omega)-$norm for $\boldsymbol{\sigma}_h$. Additionally, we proved that refining only the second-level mesh leads to optimal convergence order of $\mathcal{O}(h^{\ell+1})$ ($\mathcal{O}(h^{m+1})$ when considering a conforming mesh)

for the $L^2(\Omega)-$norm of $\Pi_{\Omega,m}(\nabla \cdot \boldsymbol{\sigma}_h)$, which contrasts to the conventional approach of using $-A\nabla u_{Hh}$ in the MHM method, for which optimal convergence does not occur.

Finally, we have proposed a fully computable *a posteriori* error estimator using both the approximate solution u_{Hh} and the approximate flux $\boldsymbol{\sigma}_h$ derived from the flux recovery strategy. The *a posteriori* error estimate provides a strict, fully computable, upper bound for the error $u - u_{Hh}$. Under mild extra regularity assumption, it also provides a lower bound for the error.

Appendix A. Technical results

Let $b_\mathfrak{f}$ be the bubble function with support in $\omega_\mathfrak{f} \in \mathcal{F}_h^K$ defined with respect to the barycentric coordinates (see for instance [3, Section 2.3.1] for details. For the sake of completeness, we line up the following theorem that summarizes the main properties of these functions.

Theorem A.1. *Let $\mathfrak{f} \in \mathcal{F}_h^K$ be a facet and let $b_\mathfrak{f}$ be the corresponding bubble function. Then there exists a positive constant C such that for all $v \in \mathbb{P}_t(T), t \geq 0$, the following holds*

$$C^{-1}\|v\|_{0,\mathfrak{f}}^2 \leq (b_\mathfrak{f} v, v)_\mathfrak{f} \leq C\|v\|_{0,\mathfrak{f}}^2\,, \tag{A.1}$$

and

$$h_T^{-1/2}\|b_\mathfrak{f} v\|_{0,T} + h_T^{1/2}|b_\mathfrak{f} v|_{1,T} \leq C\|v\|_{0,\mathfrak{f}}\,, \tag{A.2}$$

where the constant C is independent of v and h_T.

We will define some notations in each subelement $T \in \mathscr{T}_h^K$ and on each subface $\mathfrak{f} \in \mathcal{F}_h^K \cap \mathcal{F}_T$, particularly, regarding internal faces. They are the following:

$$R_T := (f + \nabla \cdot A\nabla u_{Hh})|_T \quad \forall\, T \in \mathscr{T}_h^K\,, \tag{A.3}$$

and on $\mathfrak{f} \in \mathcal{F}_0^K \cap \mathcal{F}_T$,

$$R_\mathfrak{f} := \left(A\nabla u_{Hh} + \pi_T^{\mathcal{RT}_\ell}\boldsymbol{\sigma} + [\![A\nabla u_{Hh}]\!]\right)\cdot \boldsymbol{n}_\mathfrak{f}\,. \tag{A.4}$$

Theorem A.2. *Let $K \in \mathscr{P}$. For $T \in \mathscr{T}_h^K$ the following holds*

$$\|R_T\|_{0,T} \leq C_A h_T^{-1}|u - u_{Hh}|_{1,T}\,. \tag{A.5}$$

Furthermore, for $\mathfrak{f} \in \mathcal{F}_0^K \cap \mathcal{F}_T$ we have that

$$\|R_\mathfrak{f}\|_{0,\mathfrak{f}} \leq C\sum_{T\in\omega_\mathfrak{f}}\left(h_T^{1/2}\|R_T\|_{0,T} + C_A h_T^{-1/2}|u - u_{Hh}|_{1,T}\right)\,, \tag{A.6}$$

where C is a positive constant independent of H and h.

Proof. Let $K \in \mathscr{P}$, $T \in \mathscr{T}_h^K$ and $\mathfrak{f} \in \mathcal{F}_h^K \cap \mathcal{F}_T$. We define $\beta_\mathfrak{f} := b_\mathfrak{f} P_\mathfrak{f}(R_\mathfrak{f})$, where $P_\mathfrak{f} : \mathbb{P}_k(\mathfrak{f}) \to \mathbb{P}_k(\omega_\mathfrak{f})$ is an extension of functions defined on a face $\mathfrak{f}$ to the patch $\omega_\mathfrak{f} = T \cup T'$. The proof of (A.5) follows identical steps to those from [5, Theorem 4.3]

Let $\mathfrak{f} \in \mathcal{F}_0^K \cap \mathcal{F}_T$, then

$$(R_\mathfrak{f}, \beta_\mathfrak{f})_\mathfrak{f} = \underbrace{(A\nabla u_{Hh} + \pi_T^{\mathcal{RT}_\ell}\boldsymbol{\sigma}\cdot\boldsymbol{n}_\mathfrak{f}, \beta_\mathfrak{f})_\mathfrak{f}}_{(a)} + \underbrace{([\![A\nabla u_{Hh}]\!]\cdot\boldsymbol{n}_\mathfrak{f}, \beta_\mathfrak{f})_\mathfrak{f}}_{(b)}\,.$$

For (a), using that $\beta_{\mathfrak{f}}|_{\partial T\setminus\mathfrak{f}}=0$ integration by parts and (A.3) we get

$$\begin{aligned}((A\nabla u_{Hh}+\pi_T^{\mathcal{RT}_\ell}\boldsymbol{\sigma})\cdot\boldsymbol{n}_{\mathfrak{f}},\beta_{\mathfrak{f}})_{\mathfrak{f}} &= \sum_{T\in\omega_{\mathfrak{f}}}(\nabla\cdot A\nabla u_{Hh},\beta_{\mathfrak{f}})_T+(A\nabla u_{Hh},\nabla\beta_{\mathfrak{f}})_T\\ &\quad+(\pi_T^{\mathcal{RT}_\ell}\boldsymbol{\sigma}\cdot\boldsymbol{n}_{\mathfrak{f}},\beta_{\mathfrak{f}})_{\partial T}\\ &= \sum_{T\in\omega_{\mathfrak{f}}}(\nabla\cdot A\nabla u_{Hh}+f,\beta_{\mathfrak{f}})_T+(A\nabla u_{Hh},\nabla\beta_{\mathfrak{f}})_T\\ &\quad+(\nabla\cdot A\nabla u,\beta_{\mathfrak{f}})_T+(\pi_T^{\mathcal{RT}_\ell}\boldsymbol{\sigma}\cdot\boldsymbol{n}_{\mathfrak{f}},\beta_{\mathfrak{f}})_{\partial T}\\ &= \sum_{T\in\omega_{\mathfrak{f}}}(R_T,\beta_{\mathfrak{f}})_T+(A\nabla(u_{Hh}-u),\nabla\beta_{\mathfrak{f}})_T\\ &\quad+((A\nabla u+\pi_T^{\mathcal{RT}_\ell}\boldsymbol{\sigma})\cdot\boldsymbol{n}_{\mathfrak{f}},\beta_{\mathfrak{f}})_{\partial T}\\ &= \sum_{T\in\omega_{\mathfrak{f}}}(R_T,\beta_{\mathfrak{f}})_T+(A\nabla(u_{Hh}-u),\nabla\beta_{\mathfrak{f}})_T\,.\end{aligned}$$

For (b), using (2.6), integration by parts, and (A.3) we get

$$\begin{aligned}(\llbracket A\nabla u_{Hh}\rrbracket\cdot\boldsymbol{n}_{\mathfrak{f}},\beta_{\mathfrak{f}})_{\mathfrak{f}} &= (A\nabla u_{Hh}|_T\cdot\boldsymbol{n}_{\mathfrak{f}}-A\nabla u_{Hh}|_{T'}\cdot\boldsymbol{n}_{\mathfrak{f}},\beta_{\mathfrak{f}})_{\mathfrak{f}}\\ &= \sum_{T\in\omega_{\mathfrak{f}}}(R_T,\beta_{\mathfrak{f}})_T+(A\nabla u_{Hh},\nabla\beta_{\mathfrak{f}})_T+(\nabla\cdot A\nabla u,\beta_{\mathfrak{f}})_T\\ &= \sum_{T\in\omega_{\mathfrak{f}}}(R_T,\beta_{\mathfrak{f}})_T+(A\nabla(u_{Hh}-u),\nabla\beta_{\mathfrak{f}})_T\,.\end{aligned}$$

Therefore, using the above bounds for (a) and (b), Cauchy-Schwarz inequality, the definition of $\beta_{\mathfrak{f}}^K$, (A.2) and stability of the operator $P_{\mathfrak{f}}$, we get

$$\begin{aligned}\|R_{\mathfrak{f}}\|_{0,\mathfrak{f}}^2 &\le C\sum_{T\in\omega_{\mathfrak{f}}}\|R_T\|_{0,T}\|\beta_{\mathfrak{f}}\|_{0,T}+\sum_{T\in\omega_{\mathfrak{f}}}C_A|u-u_{Hh}|_{1,T}|\beta_{\mathfrak{f}}|_{1,T}\\ &\le C\sum_{T\in\omega_{\mathfrak{f}}}\|R_T\|_{0,T}h_T^{1/2}\|R_{\mathfrak{f}}\|_{0,\mathfrak{f}}+\sum_{T\in\omega_{\mathfrak{f}}}C_A|u-u_{Hh}|_{1,T}h_T^{-1/2}\|R_{\mathfrak{f}}\|_{0,\mathfrak{f}}\\ &\le C\sum_{T\in\omega_{\mathfrak{f}}}\left\{h_T^{1/2}\|R_T\|_{0,T}+C_Ah_T^{-1/2}|u-u_{Hh}|_{1,T}\right\}\|R_{\mathfrak{f}}\|_{0,\mathfrak{f}}\,,\end{aligned}$$

which finishes the proof. □

Acknowledgments

We would like to acknowledge the IPES research group (http://ipes.lncc.br/) for the valuable discussions and CNPq/Brazil and The London Mathematical Society for funding this research.

Funding

We would like to acknowledge the IPES research group (http://ipes.lncc.br/) for the valuable discussions and CNPq/Brazil and The London Mathematical Society for funding this research. This work was authored in part by the National Renewable Energy Laboratory, operated by Alliance for Sustainable Energy, LLC, for the U.S. Department of Energy (DOE) under Contract No. DE-AC36-08GO28308. The views expressed in the presentation do not necessarily represent the views of the DOE or the U.S. Government. The U.S. Government retains and the publisher, by accepting the article for publication, acknowledges that the U.S. Government retains a nonexclusive, paid-up, irrevocable, worldwide license to publish or reproduce the published form of this work, or allow others to do so, for U.S. Government purposes.

References

[1] A. Abdulle, W. E, B. Engquist, and E. Vanden-Eijnden. The heterogeneous multiscale methods. *Communications in Mathematical Sciences*, 1 (1):87–132, 2003.

[2] Y. Achdou, C. Bernardi, and F. Coquel. A priori and a posteriori analysis of finite volume discretizations of Darcy's equations. *Numerische Mathematik*, 96:17–42, 2003.

[3] M. Ainsworth and J.T. Oden. A posteriori error estimation in finite element analysis. *Computer Methods in Applied Mechanics and Engineering*, 142(1):1–88, 1997. ISSN 0045-7825.

[4] R. Araya, C. Harder, D. Paredes, and F. Valentin. Multiscale hybrid-mixed method. *SIAM Journal on Numerical Analysis*, 51(6):3505–3531, 2013.

[5] R. Araya, R. Rebolledo, and F. Valentin. On a multiscale a posteriori error estimator for the Stokes and Brinkman equations. *IMA Journal of Numerical Analysis*, 41(1):344–380, 2021.

[6] T. Arbogast, G. Pencheva, M. F. Wheeler, and I. Yotov. A multiscale mortar mixed finite element method. *SIAM Multiscale Modeling and Simulation*, 6:319–346, 2007.

[7] I. Babuska and E. Osborn. Generalized finite element methods: Their performance and their relation to mixed methods. *SIAM J. Num. Anal.*, 20(3):510–536, 1983.

[8] G. R. Barrenechea, L. P. Franca, and F. Valentin. A Petrov–Galerkin enriched method: A mass conservative finite element method for the Darcy equation. *Computer Methods in Applied Mechanics and Engineering*, 196 (21-24):2449–2464, 2007.

[9] G. R. Barrenechea, F. Jaillet, D. Paredes, and F. Valentin. The multiscale hybrid mixed method in general polygonal meshes. *Numerische Mathematik*, 145(1):197–237, 2020.

[10] Gustavo Alcalá Batistela, Denise de Siqueira, Philippe R. B. Devloo, and Sônia M. Gomes. A posteriori error estimator for a multiscale hybrid mixed method for Darcy's flows. *International Journal for Numerical Methods in Engineering*, 123(24):6052–6078, 2022.

[11] E. Burman and A. Ern. Continuous interior penalty *hp*-finite element methods for advection and advection-diffusion equations. *Mathematics of computation*, 76(259):1119–1140, 2007.

[12] Z. Cai and S. Zhang. Flux recovery and a posteriori error estimators: conforming elements for scalar elliptic equations. *SIAM journal on numerical analysis*, 48(2):578–602, 2010.

[13] S.H. Chou, D. Kwak, and K. Kim. Flux recovery from primal hybrid finite element methods. *SIAM Journal on Numerical Analysis*, 40(2):403–415, 2002.

[14] M. A. Christie and M. J. Blunt. Tenth SPE comparative solution project: A comparison of upscaling techniques. In *SPE Reservoir Simulation Symposium*. Society of Petroleum Engineers, 2001.

[15] M. R. Correa and G. Taraschi. Optimal H(div) flux approximations from the primal hybrid finite element method on quadrilateral meshes. *Computer Methods in Applied Mechanics and Engineering*, 400:115539, 2022. ISSN 0045-7825.

[16] Ricardo G. Durán. *Mixed finite element methods*, pages 1–44. Springer Berlin Heidelberg, Berlin, Heidelberg, 2008.

[17] O. Durán, P. R.B. Devloo, S. M. Gomes, and F. Valentin. A multiscale hybrid method for Darcy's problems using mixed finite element local solvers. *Computer Methods in Applied Mechanics and Engineering*, 354:213–244,

2019. ISSN 0045-7825.

[18] Y. Efendiev, T.Y. Hou, and X.H. Wu. Convergence of a nonconforming multiscale finite element method. *SIAM J. Numer. Anal.*, 37(3):888–910, 2000.

[19] A. Ern and J.L. Guermond. *Finite elements I: Approximation and interpolation*, volume 72. Springer Nature, 2021.

[20] A. Ern and M. Vohralík. Flux reconstruction and a posteriori error estimation for discontinuous Galerkin methods on general nonmatching grids. *Comptes Rendus Mathematique*, 347(7):441–444, 2009. ISSN 1631-073X.

[21] A. Ern, S. Nicaise, and M. Vohralík. An accurate H(div) flux reconstruction for discontinuous Galerkin approximations of elliptic problems. *Comptes Rendus Mathematique*, 345(12):709–712, 2007.

[22] Alexandre Ern, Annette F. Stephansen, and Martin Vohralík. Guaranteed and robust discontinuous Galerkin a posteriori error estimates for convection–diffusion–reaction problems. *Journal of Computational and Applied Mathematics*, 234(1):114–130, 2010. ISSN 0377-0427.

[23] H. Fernando, C. Harder, D. Paredes, and F. Valentin. Numerical multiscale methods for a reaction-dominated model. *Computer Methods in Applied Mechanics and Engineering*, 201:228–244, 2012.

[24] A. T. A. Gomes, W. S. Pereira, and F. Valentin. The MHM method for linear elasticity on polytopal meshes. *IMA Journal of Numerical Analysis*, 43(4):2265–2298, 08 2022. ISSN 0272-4979.

[25] C. Harder and F. Valentin. Foundations of the MHM method. In G. R. Barrenechea, F. Brezzi, A. Cangiani, and E. H. Georgoulis, editors, *Building Bridges: Connections and Challenges in Modern Approaches to Numerical Partial Differential Equations*, Lecture Notes in Computational Science and Engineering, Edinburgh, 2016. Springer.

[26] C. Harder, D. Paredes, and F. Valentin. A family of multiscale hybrid-mixed finite element methods for the Darcy equation with rough coefficients. *J. Comput. Phys.*, 245:107–130, 2013.

[27] F. Hecht. New development in FreeFem++. *J. Numer. Math.*, 20(3-4): 251–265, 2012. ISSN 1570-2820.

[28] T. JR Hughes, G. R Feijó, L. Mazzei, and J.B. Quincy. The variational multiscale method—a paradigm for computational mechanics. *Computer methods in applied mechanics and engineering*, 166(1-2):3–24, 1998.

[29] O. A. Karakashian and F. Pascal. A posteriori error estimates for a discontinuous Galerkin approximation of second-order elliptic problems. *SIAM Journal on Numerical Analysis*, 41(6):2374–2399, 2003.

[30] A. Loula, F. Rochinha, and M. Murad. Higher-order gradient post-processings for second-order elliptic problems. *Computer Methods in Applied Mechanics and Engineering*, 128(3-4):361–381, 1995.

[31] A. Målqvist and D. Peterseim. *Numerical homogenization by localized orthogonal decomposition*, volume 5 of *SIAM Spotlights*. Society for Industrial and Applied Mathematics (SIAM), Philadelphia, PA, 2021. ISBN 978-1-611976-44-1.

[32] A.L. Madureira and M. Sarkis. Hybrid localized spectral decomposition for multiscale problems. *SIAM Journal on Numerical Analysis*, 59(2): 829–863, 2021.

[33] A. Malqvist and D. Peterseim. Localization of elliptic multiscale problems. *Math. Comp.*, 83(290):2583–2603, 2014.

[34] P. Oswald. On a bpx-preconditioner for P1 elements. *Computing (Wien. Print)*, 51(2):125–133, 1993.

[35] P.A. Raviart and J.M. Thomas. Primal hybrid finite element methods for 2nd order elliptic equations. *Math. Comp.*, 31(138):391–413, 1977.

[36] W. Zheng and H. Qi. On Friedrichs–Poincaré-type inequalities. *Journal of Mathematical Analysis and Applications*, 304(2):542–551, 2005. ISSN 0022-247X.

[37] O. C. Zienkiewicz and J. Z. Zhu. The superconvergent patch recovery and a posteriori error estimates. part 1: The recovery technique. *International Journal for Numerical Methods in Engineering*, 33(7):1331–1364, 1992.

(GRB) Department of Mathematics and Statistics, University of Strathclyde, Glasgow, Scotland, gabriel.barrenechea@strath.ac.uk

(LM) Department of Mathematical and Computational Methods, LNCC, Petrópolis, RJ, Brazil larissam@posgrad.lncc.br

(WSP) Computational Science Center, National Renewable Energy Laboratory, CO, US wdasilv@nrel.gov

(FV) Department of Mathematical and Computational Methods, LNCC, Petrópolis, RJ, Brazil valentin@lncc.br